

BI Norwegian Business School - campus Oslo

GRA 19703

Master Thesis

Thesis Master of Science

The Social Cost of Carbon from Permafrost Infrastructure
Damage and Carbon Feedback Under Climate Change

Navn: Abhijeet Kumar Singh, Andželika
Medvedeva

Start: 15.01.2021 09.00

Finish: 01.07.2021 12.00

Master Thesis

The Social Cost of Carbon from Permafrost Infrastructure Damage and Carbon Feedback Under Climate Change

Authors:

Andželika Medvedeva and Abhijeet Kumar Singh

Supervisor:

Auke Hunneman

Programme:

Master of Science in Business Analytics

June 2021, BI Oslo

Acknowledgements

This thesis marks the end of our MSc in Business Analytics programme at BI Norwegian Business School. We sincerely thank our Supervisor, Auke Hunneman, for the thoughtful guidance and enthusiasm during our research process. We also thank our friends and family for their support.

Abstract

This research determined the Social Cost of Carbon (SCC) from the combined module comprising permafrost infrastructure damage and carbon feedback under climate change. Climate change is a crisis that requires international cooperation of governments and corporations to reduce carbon emissions by including the cost of carbon into the decision-making strategies. The study was performed using the DICE-2016R integrated assessment model that incorporated emissions from the merged element of permafrost carbon feedback and additional GHG from permafrost infrastructure damage to estimate the SCC. The optimisation analysis that maximized a social welfare function found that the SCC was higher by 6-24% until 2100 than current predictions due to the combined effect of permafrost and infrastructure damages, contributing to an extra 110 trillion US dollars by the year 2200. The research showed that current SCC values are underestimated, leading to a lack of green innovation to reduce emissions and tackle climate change. We propose to include the permafrost and infrastructure module in future integrated assessment models and to set the higher SCC and increase it over time for policymakers and businesses to foster clean technologies and mitigate future climate damages.

Keywords: Social Cost of Carbon, climate change, permafrost, infrastructure.

Table of Contents

1. INTRODUCTION	1
2. LITERATURE REVIEW	3
2.1. EFFECTS OF CLIMATE CHANGE.....	3
2.2. POLICIES TO REDUCE EMISSIONS.....	4
2.3. IAMs TO QUANTIFY CLIMATE CHANGE EFFECTS.....	5
2.4. DICE AND SOCIAL COST OF CARBON.....	8
2.5. SCC FOR LOW-CARBON TRANSITION AND INNOVATION IN BUSINESS.....	9
2.6. UNDERESTIMATION OF SCC IN IAMs AND IMPORTANCE OF PCF&I	11
2.6.1. Permafrost Aspect.....	12
2.6.2. Infrastructure Aspect	13
2.6.3. PCF&I Combined	15
3. METHODOLOGY	17
3.1. MODELLING.....	17
3.1.1. Phase 1: Permafrost Thawing Model and Data.	18
3.1.2. Phase 2: GHG from Permafrost and Infrastructure Damages	20
3.1.3. Adding Permafrost and Infrastructure GHG to DICE-2016R	32
4. RESULTS AND DISCUSSION.....	34
4.1. PERMAFROST AND INFRASTRUCTURE EFFECTS	34
4.1.1. Infrastructure Carbon Emissions	34
4.1.2. Permafrost Carbon Emissions.....	36
4.1.3. Combined Environmental Impact.....	37
4.1.4. Combined Economic Impact	40
4.2. SENSITIVITY ANALYSIS OF SCC FOR 2025	43
4.3. IMPLICATIONS OF SCC FOR BUSINESSES.....	44
5. CONCLUSION	45
6. LIMITATIONS AND FUTURE RESEARCH	46
REFERENCES	47

List of Tables

Table 1. <i>SCC (2007 USD per CO₂ ton) (United States Government, 2010).</i>	9
Table 2. <i>SCC (2010 USD per CO₂ ton) (Nordhaus, 2017a).</i>	9
Table 3. <i>Permafrost and Climate Change Models.</i>	13
Table 4. <i>Permafrost and Infrastructure Damage Models.</i>	15
Table 5. <i>Regression of Permafrost Thaw.</i>	19
Table 6. <i>Estimates of Permafrost Carbon Pool (0-3m) (Kessler, 2017).</i>	20
Table 7. <i>Estimates of Relative Size of the Stagnant Pool (Kessler, 2017).</i>	20
Table 8. <i>E-folding of Permafrost Carbon Decomposition (Kessler, 2017).</i>	23
Table 9. <i>Permafrost Extent Attributes.</i>	27
Table 10. <i>Settlement Extent.</i>	28
Table 11. <i>Night-time Light.</i>	29
Table 12. <i>Formulae for Radiative Forcing (RF) from CH₄ and N₂O.</i>	33
Table 13. <i>Masked Area for Settlement and Nigh-time light.</i>	35
Table 14. <i>Social Cost of Carbon DICE-2016R (2010 US\$).</i>	42
Table 15. <i>SCC 2025 (2010 US\$) Sensitivity Analysis.</i>	43

List of Figures

Figure 1. <i>Climate-Economy Generalized Model (Nikas et al., 2019).</i>	6
Figure 2. <i>Permafrost Extent Layer Image.</i>	28
Figure 3. <i>Settlement Layer Image (Partial).</i>	29
Figure 4. <i>Night-light Layer Image (Partial).</i>	30
Figure 5. <i>DICE Model Simplified Representation.</i>	32
Figure 6. <i>Permafrost Layer.</i>	35
Figure 7. <i>Settlement Layer.</i>	35
Figure 8. <i>Night-light Layer.</i>	35
Figure 9. <i>Masked - All Layers.</i>	35
Figure 10. <i>Permafrost Extent.</i>	36
Figure 11. <i>Carbon from Permafrost.</i>	36
Figure 12. <i>Radiative Forcing.</i>	37
Figure 13. <i>Emissions.</i>	37
Figure 14. <i>TATM.</i>	37
Figure 15. <i>MAT.</i>	37
Figure 16. <i>Damages.</i>	40
Figure 17. <i>Control Rate.</i>	40
Figure 18. <i>Investment.</i>	40
Figure 19. <i>Consumption.</i>	40
Figure 20. <i>Carbon Price in 2010US\$.</i>	42
Figure 21. <i>SCC in 2010US\$.</i>	42

1. Introduction

The global climate has undergone warming during the last century and is projected to proceed warming in the next 100 years (Collins et al., 2013). To incentivise the actions and counteract the climate warming effects, we need to estimate its economic impact in order to justify a global call for action for policymakers, businesses and the public. Currently, Integrated Assessment Models (IAMs) help to quantify the effect caused by Greenhouse Gas (GHG) emissions by determining the Social Cost of Carbon (SCC). The IAMs combine different scientific and economic spheres and integrate the interconnected models of damages, climate, energy and economy altogether (Hare et al., 2018). The output of IAMs is SCC - an economic measure that assesses climate change's marginal costs of externality in a monetized value from an increase of 1 metric ton of carbon dioxide emissions (National Academies of Sciences, Engineering, and Medicine, 2017). The cost enables governments and businesses to reduce pollution by incorporating the environmental costs and benefits into policies, strategies and decision-making processes. Carbon cost is a driving force contributing to the transition to a low-carbon future by incentivizing investments in innovations aimed at reducing emissions.

However, the SCC is severely underestimated in the IAMs since essential variables such as various climate effects, risk and indirect effects are not included to contribute to climate change damages (Howard & Schwartz, 2016; Mastrandrea, 2009; National Academies of Sciences, Engineering, and Medicine, 2017; Than, 2015). In this study, there are two important limitations of IAMs that we focus on – permafrost carbon feedback and infrastructure effects caused by permafrost thaw.

Permafrost carbon feedback (PCF) is studied but seldom included in the IAMs even though it causes a 6-21% increase in costs to tackle carbon emissions (González-Eguino & Neumann, 2016). Our estimates suggest that the costs are even higher with infrastructure included (6-24% until 2100). The infrastructure damages from flooding might be included in the cost calculations of SCC in IAMs, but damages from permafrost are not taken into consideration (National Academies of Sciences, Engineering, and Medicine, 2017). The rebuilding of this infrastructure would require additional investments and also would emit GHG. Moreover, even though some distinct aspects of permafrost effects, such as its ability to emit additional GHG and affect nature and humans, have been incorporated into IAMs, permafrost and infrastructure aspects are never merged in the IAM.

Hence, our suggested model includes both permafrost carbon feedback and infrastructure effects. The research question in this thesis asks what the increase in SCC is by incorporating the carbon release from permafrost infrastructure damage and carbon feedback from permafrost thaw in the realm of climate change. The IAM chosen to calculate the SCC is the Dynamic Integrated model of Climate and the Economy (DICE¹) model developed by an economist and 2018 Nobel Prize recipient William Nordhaus. DICE is one of the most significant and transparent IAMs and is also used by the United States government (United States Government, 2010, 2016). We use the latest version of the model (DICE 2016-R). It estimates the SCC in monetary value (Nordhaus, 2017b). By incorporating the most recent data of permafrost, we estimate the new, more inclusive and accurate SCC that is widely used by policymakers and businesses.

We show that, as a result, the SCC is highly underestimated. The economic impact is much more prominent when permafrost and infrastructure are included. According to our research, the SCC due to permafrost and infrastructure emissions increases between 6-24% until 2100. The implications stemming from the underestimation of SCC is that there is a lack of eco-innovation. To foster green innovation, SCC should be increased to become the catalyst for more clean technologies since they are more viable to invest in.

¹ A full description of the equations and parameters of the DICE model is available in the DICE User's Manual (Nordhaus & Sztorc, 2013).

2. Literature Review

2.1. Effects of Climate Change

Over the past 20 years, 18 were the hottest years on record, and after going over one extra degree in average temperature, the global warming level increases by 0.2°C every 10 years (European Commission, 2018). The increasing temperature causes permanent climate effects that can be irreversible, with a substantial negative impact on ecosystems and economies. Media, news and scientists recommend changing the language around climate change, naming it a climate crisis, to incentivize people to take action and inform them about the current situation that has to be solved (Rigby, 2020). Global warming affects the environment by making extreme weather events like wildfires, floods, hurricanes, and permafrost thaw stronger and more frequent. Climate change is expected to affect geophysical, biological, and socioeconomic systems (F. Li et al., 2015; Liu et al., 2012; Schneider et al., 2007; Huijun Wang et al., 2015; Huijun Wang & Sun, 2009). With the 2°C temperature increase compared to pre-industry levels, the impact includes the loss of almost all coral reefs, the disappearance of Greenland glacial ice and Arctic sea ice, rising sea level to 7 meters, negative influence on wildlife, human population, economy, infrastructure, and political stability (European Commission, 2018). According to B. Gates (2021), the Intergovernmental Panel on Climate Change (IPCC) claims that two additional degrees added to the average temperature would contribute to a loss of 8% of vertebrates, 16% of plants and 18% of insects. It is stated that “the economic damage caused by climate change will likely be as bad as having a COVID-sized pandemic every 10 years” (Gates, 2021, p. 37). In the US, it is estimated to cost 0.7% - 1% of GDP per year (Gates, 2021).

That being said, climate warming has not been globally consistent. Higher warming is observed and predicted to occur in higher northern latitudes and high-altitude areas (Collins et al., 2013; Guo & Wang, 2012; Hartmann et al., 2013; Zhou et al., 2014, 2016). Therefore, regional climate changes are anticipated to differ. It is predicted that the Arctic is enduring a warming rate that is exceeding double the global one (WMO et al., 2020). Permafrost, by definition, is the ground where soil temperature remains at or below 0°C for at least two sequential years, and its thawing is a significant issue since permafrost is extensively distributed in high-latitude and high-altitude regions, where the most significant warming is predicted to occur. Permafrost near the current southern rim of its extent is degrading, and this process may include a northward shift in the south boundary of permafrost by

hundreds of kilometres throughout much of northern North America and Eurasia. As a massive carbon pool, permafrost soils store 1460 to 1600 Gt of organic carbon, almost twice the carbon present in the current atmosphere (Schuur et al., 2009; WMO et al., 2020; Zimov et al., 2006). The released emissions from permafrost would contribute to warming at unprecedented levels.

2.2. Policies to Reduce Emissions

To tackle climate change, international coordination is crucial, and the goals to tackle global warming have been agreed upon internationally and requires the participation of corporations by reducing emissions in their operations (Bento & Gianfrate, 2020). Initiatives and regulations firstly come from politics. It is stated that we should keep the mean global warming below 2°C relative to preindustrial temperatures (UNFCCC, 1997, 2015). The Kyoto Protocol with legally binding obligations to reduce emissions was adopted in 1997 by the United Nations Framework Convention on Climate Change obligations for limits and reductions for ‘developed’ countries only (Savaresi, 2016). Afterwards, the Paris Agreement, an international treaty, was adopted in 2015 and entered into force in 2016, intending to limit global warming to under 2°C, or to 1.5°C, against pre-industrial level (Savaresi, 2016). To reach the aforementioned targets, scientists state that pricing GHG emissions is an efficient governing method using two market-based instruments – emissions trading system (ETS) and/or carbon tax (Haites, 2018).

The most common form of emissions trading system is cap-and-trade, which places a maximum amount on the aggregate GHG emissions and creates a fixed number of tradable allowances corresponding to the firm’s emissions (Stavins, 2007). In that way, the emissions are reduced at the lowest economic cost collectively since it creates incentives for companies to act most cost-effectively by either reducing the emissions and/or selling/buying the allowances. Over time, the aggregate cap is reduced to reach climate goals (Hintermayer, 2020).

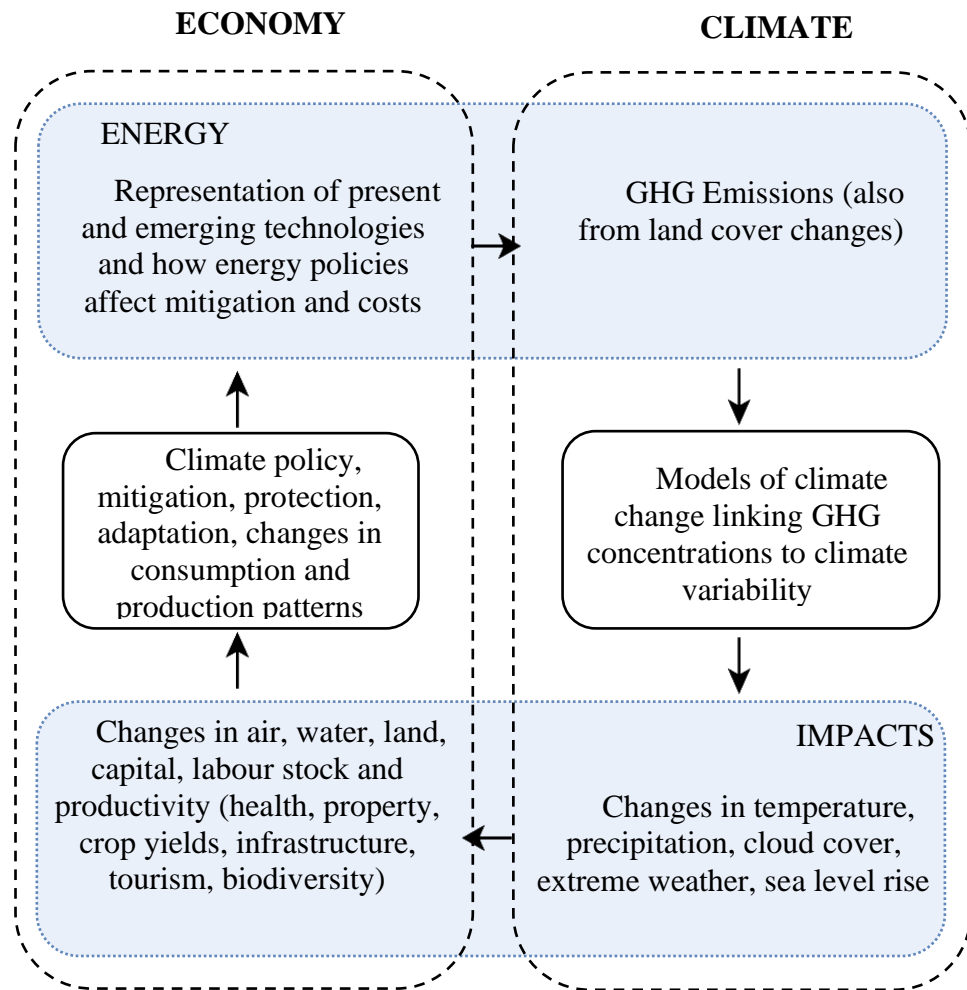
The second instrument to price GHG emissions, first implemented in Scandinavia in the 1990s, is a carbon tax, where the government puts a price on the emissions directly, and the tax rate can differ depending on the economic, technological and political environment (Partnership for Market Readiness, 2017). The initial tax rate also depends on the approach. A carbon tax can be set according to the Social Cost of Carbon (SCC), which is “one of the most economically efficient approaches” (Partnership for Market Readiness, 2017, p. 89).

Weitzman (2017) argues that climate change is one of the toughest negative public-good externalities, and there is no worldwide mechanism that deals with the free-riding issue. Notwithstanding the Kyoto Protocol and Paris Agreement, none of them have dealt with free-riding since there is no punishment for setting too low national targets despite the reputation that it is not effective enough to reduce the emissions drastically as needed (Weitzman, 2017). Thus, scholars propose to negotiate a uniform minimum worldwide carbon price to incentivize the participants to internalize the climate change effects (Goller & Tirole, 2015; Stiglitz, 2015; Weitzman, 2017). Agreeing on one global carbon price is relatively simple compared to finding several prices (Weitzman, 2017). This idea was first reflected in Nordhaus (2015), where the author proposed a ‘Climate Club’. The club comprises the participating countries that establish relevant domestic policies to reach the goals with the negotiated minimum carbon price, and non-participants are penalized. Although the uniform carbon price is difficult to achieve politically, it is more effective economically (Hovi et al., 2019). This solution is still proposed by Nordhaus (2019, 2020). Hence, coordination is needed to find one value of the Social Cost of Carbon (SCC) globally.

2.3. IAMs to Quantify Climate Change Effects

In order to find SCC, Integrated assessment models (IAMs) are used. IAMs are the cornerstone of quantifying the human impact on climate change and informing governments, corporations and the public so that emissions are reduced. Integrated Assessment Models are progressively used in international policy decisions to determine the impact of economic activity on the environment, assess the costs-benefits of policies and technological research strategies (Nordhaus, 2017a). IAMs incorporate different spheres and domains of knowledge, integrating impacts, climate, energy and economy (Hare et al., 2018; Nordhaus, 2017a; Schwanitz, 2013). That helps to combine the climate-economic feedback dynamics. The generalized model (Nikas et al., 2019) is shown in Figure 1.

Figure 1. *Climate-Economy Generalized Model (Nikas et al., 2019).*



The economy modelling comes from the market-based economic processes and theories about economic growth (Hare et al., 2018). The energy model, initially concentrated on predicting the fossil fuels and nuclear power supply and demand equilibria, eventually transformed into an integrated model by including a component of an emissions model, which later followed by a carbon cycle and a simple climate model (Hare et al., 2018; Nordhaus, 2017a). Now the energy model part also concentrates on the various sources and alternatives of energy and technology that contribute to reducing GHG (Nikas et al., 2019). The climate module describes the link between GHG emission, atmospheric concentrations and the resulting variation in temperature and other climatic changes (precipitation, cloud cover, extreme weather events, climate discontinuities). The impacts module (or damage function) expresses outcomes as a function of climate variables. One more element taking part in the integrated feedback is the climate science models

that consider the physics and chemistry, GHG concentration, temperature and other relevant determinants in the climate system to find optimal strategies of GHG mitigation (Hare et al., 2018). The impacts or damages take into consideration the future consequences from climate variables since emissions today can have economic consequences for the following centuries (National Academies of Sciences, Engineering, and Medicine, 2017; Nikas et al., 2019).

Because climate change models are complex and have a lot of interdependent systems with the global economy, Metcalf and Stock (2015) focus on three crucial elements that are very sensitive and can influence the models' outcomes to a large extent. Critical areas are damage functions, climate sensitivity and the discount rate. The initial damage functions in IAMs were 'top-down', taking into account the relationship between GDP and temperature; however, it is suggested that a 'bottom-up' methodology should be considered such as property damage costs due to hurricanes, storms and higher sea-level (Metcalf & Stock, 2015). The damage function conveys the temperature, and other climate features into the economic effects, and usually, the simple generalized form of damage function is:

$$D = aT^b \quad (1)$$

Where D is the monetary or % of output damage value, T is the temperature difference between periods and exponent b defines the curve's shape or steepness (Stanton et al., 2009). Thus, the steepness can suggest the likelihood of climate catastrophe that leads to another point of sensitive elements in the IAMs. Climate sensitivity to catastrophe comprises the 'tipping' points, the irrevocable climate change effects, comprising melting Arctic sea ice and a positive feedback loop of GHG emissions from thawing permafrost (Metcalf & Stock, 2015; National Academies of Sciences, Engineering, and Medicine, 2017). The last sensitive point in estimating the model's output such as SCC is discount rate $r(t)$ which includes two components of the pure rate of social time preference ρ and the growth rate of GDP per capita, $g(t)$ with the marginal utility elasticity η (Stanton et al., 2009):

$$r(t) = \rho + \eta g(t) \quad (2)$$

To create a common ground for scientists and economists, some models have to be simplified. Three most popular and influential, but simpler IAMs that are used by policymakers include Dynamic Integrated model of Climate and the Economy (DICE), The Climate Framework for Uncertainty, Negotiation and Distribution

(FUND), and Policy Analysis for the Greenhouse Effect (PAGE) (Calel & Stainforth, 2017). They all take into account the above mentioned economic and climate elements to quantify the price of carbon.

2.4. DICE and Social Cost of Carbon

In this thesis, we focus and use one of the three models mentioned before, and it is the DICE model, developed by William Nordhaus, due to the model's transparency and many updates and resources such as documentation, journals, books and articles provided by the author (Metcalf & Stock, 2015; Nordhaus, 2017b, 2019, 2020).

The latest version of DICE is DICE-2016R². The DICE model puts the climate change in the perspective of neoclassical economic growth theory, specifically, the Ramsey model³, where people save and invest in capital goods that result in redistributing more of their present consumption into their future consumption (Nordhaus, 2017b). Thus, Nordhaus incorporates climate investments into the capital good in the Ramsey model (Nordhaus, 2017b). Nordhaus modifies Ramsey's model to include climate investments instead of capital investments only. Therefore, the investment and damages outputs are also vital in quantifying the climate change effects. Then, DICE calculates the Social Cost of Carbon (SCC) which is the most crucial economic concept in climate change economics (Nordhaus, 2017b).

To illustrate the current valuations of the SCC, we look into the US case. The US government uses SCC, and the rates are provided in the Technical Update of the Social Cost of Carbon for Regulatory Impact Analysis by United States Government's Interagency Working Group on Social Cost of Greenhouse Gases (United States Government, 2010, 2016). Disaggregated prices coming from the DICE model only are provided in Table 1 (discount rate of 2010).

² More about DICE and versions (including DICE-2016R) can be found at Scientific and Economic Background on DICE models (*DICE/RICE Models - William Nordhaus | Yale Economics*, 2020).

³ See (Garcia Duarte, 2008) for more about Ramsey's work.

Table 1. *SCC (2007 USD per CO₂ ton) (United States Government, 2010).*

Discount rate:		5%	3%	2.5%	3%
Model	Scenario	Avg	Avg	Avg	95th
DICE	IMAGE	10.8	35.8	54.2	70.8
	MERGE	7.5	22.0	31.6	42.1
	Message	9.8	29.8	43.5	58.6
	MiniCAM	8.6	28.8	44.4	57.9
	550 Average	8.2	24.9	37.4	50.8

However, the most updated SCC (Table 2), including the future estimates, from the DICE model is provided by Nordhaus (2017a).

Table 2. *SCC (2010 USD per CO₂ ton) (Nordhaus, 2017a).*

Scenario	2015	2020	2025	2030	2050
Base parameters					
Baseline	30.0	35.7	42.3	49.5	98.3
Optimal controls	29.5	35.3	41.8	49.2	99.6
2.5 degree maximum					
Maximum	184.1	229.0	284.0	351.0	1 008.4
Max. for 50 years	147.2	183.2	227.2	280.4	615.6
Stern Review discounting					
Uncalibrated	256.5	299.6	340.7	381.7	615.5
Alternative discount rates					
2.5%	111.1	133.4	148.7	162.3	242.6
3%	71.6	85.3	94.4	104.0	161.7
4%	34.0	39.6	44.5	49.8	82.1
5%	18.9	21.7	24.8	28.1	48.4

The SCC is used to determine not only the output of the model but also the carbon tax and internal carbon price in businesses on which we will expand on in the next section. Thus, it is crucial to have estimates of SCC, damages and climate investments as close to reality as possible to tackle climate change and plan for a future with lower GHG emissions.

2.5. SCC for Low-Carbon Transition and Innovation in Business

To reach the climate goals set by international agreements, the participation of businesses is vital. Determining a carbon price within a firm helps to internalize the

cost of GHG emissions by allocating a monetary value to every ton emitted (Ahluwalia, 2017). In that way, companies can take part in the transition to a low-carbon future by factoring carbon prices into their strategic decisions (Ahluwalia, 2017; Bento & Gianfrate, 2020). Carbon prices help to identify low-carbon and high-return investment opportunities (Fan et al., 2021). The techniques to internally price carbon in the company include a carbon fee that accounts for emissions from regular business activity, a theoretical shadow price, an implicit carbon price based on marginal abatement cost, or a hybrid of the combination of the methods (Ahluwalia, 2017). The common estimation that is used both by policy decision-makers to set a carbon tax and companies to set an internal carbon price is the Social Cost of Carbon (OECD, 2018; Price et al., 2007).

According to Carbon Disclosure Project (CDP), there is a surge in corporate carbon pricing and reporting, where the number of companies disclosing climate change grew from 228 in 2003 to 9 526 in 2020 (*Companies Scores - CDP*, n.d.). Businesses are incentivized to report the emissions due to external pressure from regulations, institutional investors and environmental groups and internal motives comprising long-term strategic planning, risk assessment, cost savings due to increasing carbon prices, brand awareness and reputational advantages (Bento & Gianfrate, 2020; Tang & Demeritt, 2018). Researchers claim that carbon pricing as corporate social responsibility (CSR), if a company is not greenwashing, not solely decreases emissions but also contributes to profitability, technological advancement and competitiveness of the company, creating a win-win result (Tang & Demeritt, 2018).

There is a positive correlation between the carbon price and climate investment since the increased price makes technologies reducing carbon emissions worth investing in (Sustainable Prosperity, 2010). With a higher cost of carbon, low-carbon energy solutions become more cost-effective and incentivize clean energy solutions if GHG emissions are integrated into companies' investment strategies (Roser, 2020; The Goldman Sachs Group, 2010). A higher carbon price incentivizes companies to reduce CO₂ as long as it is less expensive than paying for carbon, but the companies still have the freedom to choose where and how to cut emissions in their activities that also boost innovation and the shift from "dirty" to "clean" technologies (Flues & Dender, 2020). Thus, the damages from emissions very much concern businesses and their survival. In a net-zero CO₂ economy that international agreements try to achieve, only companies with net zero-carbon activities will be

competitive and increase their market share, whereas companies delaying the shift will face issues concerning physical, legal, reputational and financial risks – deteriorating revenues and values of assets (Flues & Dender, 2020).

However, currently, the Cost of Carbon in the world is not high enough (Flues & Dender, 2020; Larsen et al., 2018; Ministry of Climate and Environment, 2017). Regarding the international business cases, Microsoft Corporation internal carbon fee is priced at \$15 per metric ton, whereas Mahindra & Mahindra Ltd. uses the one priced at \$10 (Ahluwalia, 2017; B. Smith, 2020). General Motors (GM) incorporates a shadow price of \$3–\$11, which mirrors regional prices according to EU or Chinese ETS, California’s cap-and-trade or Canadian carbon tax (Ahluwalia, 2017). Shell and BP use the internal GHG price of \$40 (Ahluwalia, 2017). Equinor implements an internal carbon price of \$55 per ton in strategic decisions (Equinor, 2020). More companies internalize the carbon emissions and include them in the operations and strategy, but the levels of prices vary.

Therefore, the most important catalyst in R&D and climate investment and innovation to decrease GHG emissions is not only today’s price of CO₂ but the prospect of growing prices in the future, especially if we are not able to alleviate the climate damages from GHG in the next 100 years (Cramton et al., 2017; Martin & Kemper, 2010). The Social Cost of Carbon has to skyrocket so that any work in reducing emissions would pay off (Flues & Dender, 2020). The dramatic increase in prices is justified by the fact that if the stock of accumulated emissions in the atmosphere is relatively high, additional emissions will cause irreversible damage (Flues & Dender, 2020). In the following section, we elaborate on the underestimation of SCC by IAMs and the importance of permafrost feedback and infrastructure as the important currently lacking elements and the focal point of this thesis.

2.6. Underestimation of SCC in IAMs and Importance of PCF&I

As discussed previously, the Carbon Costs, including the SCC values in Table 1 and Table 2, are usually undervalued since it is challenging to incorporate all the relevant aspects. Even though the IAMs usually have the damage function to calculate the SCC, some important factors and risks are not included. That leads to a severe underestimation of the values in the realm of climate change damages. The Social Cost of Carbon is claimed to be underestimated ruthlessly (Howard & Schwartz, 2016; World Bank, 2017). A wider variety of climate effect determinants

is recommended to be incorporated into IAMs (Mastrandrea, 2009; National Academies of Sciences, Engineering, and Medicine, 2017).

The literature (Table 3 and Table 4) suggests that there is an underestimation of SCC due to the lack of models that incorporate permafrost carbon feedback (PCF) or infrastructure damages (I) coming from permafrost thawing into the IAMs. The permafrost is a vital participant in climate change (Nelson & Anisimov, 1993) since (1) it can act as a facilitator of distant climate change through the discharge of greenhouse gases (Goulden et al., 1998; Michaelson et al., 1996; Rivkin, 1998) and (2) it can be an active translator of environmental change through its impacts on natural and human societies (infrastructure included) (Williams, 1995).

2.6.1. Permafrost Aspect

The first aspect is the most significant contributor as the terrestrial permafrost carbon pool in the circum-Arctic permafrost regions is 1330–1580 Pg (1 Pg = 1 billion tons) (Schuur et al., 2015), nearly double that in the atmosphere (Zimov et al., 2006). A long-term rise in summer temperatures in the high northern latitudes could result in notable increases in the depth of the seasonally thawed layer above permafrost. In the Northern Hemisphere, it is estimated that permafrost spread is approximately $22.79 \times 10^6 \text{ km}^2$, which is equivalent to about 1/4 of the Northern Hemisphere land area. It is assessed that permafrost soils in the Northern Hemisphere store approximately $11.37\text{--}36.55 \times 10^3 \text{ km}^3$ of ground ice (Zhang et al., 1999). The freezing and thawing processes of the surface layers of permafrost regulate the fluctuations of soil and surface water and heat, which in turn heavily affects the soil's biogeochemical cycles, surface energy budgets, local hydrological processes, vegetation, the stability of infrastructure, and climate change (Guo et al., 2011a, 2011b; Koven et al., 2011; Q. Li & Chen, 2013; Nelson et al., 2002; Qin et al., 2014; K. Yang et al., 2014; M. Yang et al., 2010; Yi et al., 2014).

The buried sediments have amassed over thousands of years through dust deposition, alluvial sedimentation, and peat⁴ development (Schuur et al., 2008; Tarnocai et al., 2009), and are to a high degree stabilized currently by remaining frozen or waterlogged (Schädel et al., 2016). Due to the Arctic intensification of

⁴ For definition and more information about the peat, see (*Peat - an Overview | ScienceDirect Topics*, n.d.)

global warming (Cohen et al., 2014), continued warming in the 21st century will significantly raise the extent of permafrost degeneration and lead to the active layer's thickening in summer periods. By 2200, the region of Arctic permafrost will be reduced by 29–59%, and the depth of the active layer will increase by 53–97cm (Schaefer et al., 2011). Although at present the carbon flux from permafrost soils toward the atmosphere is of minute importance relative to the whole permafrost carbon pool, thawing permafrost in the Arctic throughout the 21st century will release a tremendous amount of soil carbon in the forms of CO₂ and CH₄ into the atmosphere, which can magnify the warming effect further (i.e., so-called permafrost carbon-climate feedback) (MacDougall et al., 2012). Thawing permafrost as the Arctic feedback provides a positive carbon release response and quickens climate change (Yumashev et al., 2019).

Table 3. *Permafrost and Climate Change Models.*

Author	Model Topic
(Burke et al., 2012, 2013; Koven et al., 2013; MacDougall et al., 2012; Schneider von Deimling et al., 2012; Schuur et al., 2015)	Permafrost carbon feedback and climate change
(González-Eguino & Neumann, 2016; Hope & Schaefer, 2016; Kessler, 2017)	Economic impact (carbon price, SCC) due to permafrost thaw or feedback

In Table 3, the two most prominent topics in the sphere of permafrost and climate change are the effect of permafrost carbon feedback on global warming and also the impact in economic terms such as SCC. The permafrost carbon feedback (PCF) has been scrutinized in the literature (Burke et al., 2013; MacDougall et al., 2012; Schneider von Deimling et al., 2012), but is rarely included in the IAMs even though it would cause 6-21% increase in costs in regards to carbon emissions lessening (González-Eguino & Neumann, 2016). Hope and Schaefer (2016) calculated the NPV of a 13% increase if carbon emissions from permafrost thawing are included. Therefore, it is crucial to assess the economic impacts of carbon emissions from the Circum-Arctic permafrost region.

2.6.2. Infrastructure Aspect

The second aspect is often overlooked in the IAMs as it is difficult to quantify. One major impact of permafrost thaw on societies that can be quantified is infrastructure damage. Besides the PCF, the economic costs would include the

losses related to infrastructure damages that are not incorporated by IAMs (Hope & Schaefer, 2016). The IAMs can consider only the flooding that damages infrastructure and requires rebuilding it, and permafrost damages are not studied (National Academies of Sciences, Engineering, and Medicine, 2017). There is a growing solicitude concerning the risk to human-made infrastructure caused by critical permafrost thaw. Although the permafrost regions are not densely populated, their financial standing has grown substantially in recent decades. Due to the abundant natural resources that the permafrost regions hold, economic development has expanded the human infrastructure: transportation networks, hydrocarbon extraction, communication channels, industrial plants, civil buildings, and engineering sustaining systems have increased considerably in recent decades. In regions with ice-rich permafrost, infrastructure could be damaged critically by the thaw-induced settlement of the ground surface due to climate change. The melting of ground ice in permafrost areas can end in settlement of the ground surface, altering the stability of infrastructures on permafrost (Guo & Sun, 2015; Nelson et al., 2002).

Rapid and extensive growth has had high costs in environmental and human terms (E. A. Smith & McCarter, 1997; Williams, 1986). These could be worsened severely by the impacts of global warming. For instance, the Tibetan Plateau region's population has tripled over the last 45 years (Fu & Zheng, 2000), followed by the rapid expansion of civil facilities and transportation networks (Cheng, 2002). Other examples involve the development of Prudhoe Bay in central Alaska's North Slope (Williams, 1986) and the oil fields in western Siberia (Seligman, 2000). Permafrost degeneration results in the ground surface's thaw settlement, most likely resulting in the severance of human-made infrastructure, particularly for ice-rich permafrost regions. Examples include the breakdown of a permafrost-underlain building in Norilsk in 1966, killing more than 20 people, and damage to more than 300 facilities, and a power-generating plant in Yakutsk, Russia, which was caused by thaw settlement (Nelson et al., 2002). As defined by the ground temperature, permafrost is potentially susceptible to climate change (Anisimov et al., 2001; Guo & Wang, 2013, 2014).

There is a significant amount of GHG effusion due to construction and transportation and support of infrastructure that have a notable effect on climate change. The literature examines the importance of infrastructure that contributes to GHG emissions. The GHG is emitted throughout different phases of infrastructure

development that include the construction phase (materials sourcing, excavations, manufacturing, construction), use phase (transportation, operations, maintenance) and waste management phase (replacement or dismantling) (Jowitt et al., 2012; Müller et al., 2013; Heming Wang et al., 2020). To put it into perspective, the carbon release of the existing global infrastructure in 2008 was around 122 Gt CO₂ (Müller et al., 2013). The literature also states that it is recommended to use international carbon finance mechanisms to evaluate low-carbon projects and also to define carbon metrics (Jowitt et al., 2012).

Table 4. *Permafrost and Infrastructure Damage Models.*

Author	Model Topic
(Cheng, 2002; Guo & Sun, 2015; Nelson et al., 2001)	Permafrost thaw and infrastructure damage
(Porfiriev et al., 2019; Streletskiy et al., 2019)	Permafrost thaw and economic impact of infrastructure damage due to climate change

As shown in Table 4, the most common topics about permafrost and infrastructure are that the permafrost thaw damages infrastructure and its respective economic costs. Studies fail to consider the extra reconstruction emission in their model while calculating the GHG emission due to permafrost thaw, which is magnified (due to reconstruction) by damage to human infrastructure.

2.6.3. PCF&I Combined

Although different aspects of each of these factors are studied before (Table 3 and Table 4) in the AIMs, it is never a blend of both (PCF&I), even though they are important and interconnected. The interconnectedness of PCF&I stems from the circular processes, where permafrost thawing emits GHG and contributes to more considerable carbon feedback, at the same time causing infrastructure damages that release additional GHG in all stages of reconstruction - material procurement, rebuilding, maintenance and usage. No studies emphasize the infrastructure's damage due to permafrost reconstruction emissions that contribute to climate change.

Hence, the Social Cost of Carbon is undervalued since permafrost carbon and infrastructure GHG feedback aspects are frequently overlooked. Consequently, it leads to a lack of green innovation. The aim of our thesis and our contribution to the research of quantifying the SCC is that we present a model that encompasses

both elements (permafrost carbon feedback and infrastructure damage due to permafrost reconstruction emissions) together. That makes SCC more inclusive and accurate since both aspects emit a significant amount of carbon back to the environment but disregarded in the research. A model incorporating both gives a more conclusive picture, differentiating our model from currently used ones.

Also, we add value by refining and comparing a carbon metric of SCC to the current estimations. It is of key importance since faulty estimations could exacerbate global warming (Kurtzer-Meyers, 2020). More accurate and higher SCC included in evaluations in policies and businesses foster a more rapid green shift in economies. The increase of SCC makes sustainable decisions and green innovation that tackle climate change by reducing CO₂ emissions more viable. Thus, data analytics can help to tackle climate change using better and more accurate data that lead to more precise calculations of carbon prices.

The research design and methodology to estimate the impact of permafrost carbon feedback and the carbon emissions due to reconstruction of damages of infrastructure due to permafrost on the Social Cost of Carbon are discussed in the next chapter.

3. Methodology

3.1. Modelling

Most research that provides estimates of latent permafrost carbon release over the coming centuries manifest their results in the following way: they give the total aggregate permafrost carbon discharged into the atmosphere by a definite date (e.g. 2100, 2200 or 2300) for a definite atmospheric carbon dioxide concentration pathway, specifically, one of the four Representative Concentration Pathways (RCPs). Such a characterization is mismatched with dynamic models such as DICE, in which emissions at the time (t) depend on atmospheric carbon dioxide concentration at time ($t-1$): admittedly, the concentration of atmospheric carbon dioxide influences global mean temperature directly and consequently climate changes, which then weigh on the level of output and emissions of GHG. Furthermore, utilizing a characterization of the permafrost carbon feedback in which emissions from permafrost carbon are entirely a function of atmospheric carbon dioxide concentration or global mean surface temperature would not allow us to explore the different uncertainties attached to the underlying processes of the permafrost carbon feedback. Indeed, if the warming scenario is one of the vital ambiguities, there are numerous other intricacies to explore. Finally, such an oversimplistic description of permafrost carbon release would circumvent the different geological, hydrological and climatic means at stake.

Hence, what we need is a method of permafrost carbon release, which is based on an accurate portrayal of the processes associated, but which is also fitting for incorporation in DICE-2016R and flexible enough to explore different types of ambiguities. The bulk of the published articles that intend to explain and quantify permafrost carbon discharge use a two-phase method; permafrost degradation (or thawing), ensued by disintegration of thawed (or vulnerable) permafrost and discharge into the atmosphere as carbon dioxide or methane. It is worth mentioning that only the first phase (thawing) is directly reliant on global mean temperature. As surface temperature increases, the active layer depth increases, and the soil carbon, which is no longer permanently frozen, becomes vulnerable to dissolution. The second stage (decomposition of carbon and release as carbon dioxide or methane) is essentially a function of the kind of permafrost soil that is imperilled to disintegration: as highlighted by Schuur, “on a global basis, microbial decomposition of organic matter is the dominant pathway of C return from terrestrial ecosystems to the atmosphere” (Schuur et al., 2008, p. 709), which is

expected to be the fact with carbon from thawed permafrost. The suggested modelling approach outlined below follows this two-phase procedure.

3.1.1. Phase 1: Permafrost Thawing Model and Data.

Permafrost thawing transpires when the surface temperature is over 0°C for part of the year. Its physical representation is based on the modelling of active-layer thickening, which indicates the widening depth of the seasonal freeze-thaw cycle. As near-surface soil temperatures rise with global warming, some of the permafrost soil changes state from ice to water, thus extending the layer of soil at the surface that thaws seasonally. Any precise representation of active-layer thickening via heat transfers would accordingly need to take into account the variety of landscapes that constitute permafrost soils, extremely localized hydrological processes and fine-grid predictions of climate variables such as surface temperature (including the consequence of polar amplification, which is not uniform across all permafrost areas) and precipitation patterns.

Because we are de facto restrained by the constraints of DICE, which is a simplistic and globally aggregated model, we employ a model based on existing assessments of expected permafrost thaw rather than a process-based method. Our hurdle is, consequently, to find a model for permafrost thaw, which is entirely dependent on global mean temperature, and which can be applied to the existing measures of permafrost degradation. We take an approach related to the one adopted by Griffies et al. (2011) to ascertain the sensitivity of the Northern Hemisphere sea ice sheet to global temperature change and which is based on an OLS regression of ΔI (the variation in sea ice cover) on ΔT (the variation in global mean temperature). Our OLS model, also used by Kessler (2017) for permafrost thaw, is as follows:

$$PF_{thawed}(t) = \beta \times (T_{ATM}(t) - T_{ATM}(t_0)) + \varepsilon \quad (3)$$

- $PF_{thawed}(t)$ is the permafrost extent that has thawed at time t (fraction)
- $T_{ATM}(t)$ is the global average surface temperature at time t (°C)
- t_0 stands for the initial year
- β coefficient is estimated with regression from equation (3).

Assumptions for the permafrost degradation model:

- As long as $T_{ATM}(t) = T_{ATM}(t_0)$, the amount of the permafrost area does not differ. The underlying theory is that $T_{ATM}(t_0)$ resembles an equilibrium phase in which the spread of permafrost is constant.

- The rate of permafrost degradation is a linear function of the increase in worldwide mean temperature above $TATM(t_0)$. The linearity part seems to be supported by the theory of permafrost dynamics (Schuur et al., 2015).

β coefficient is estimated based on data (103 observations) with permafrost degradation projections (RCP⁵ scenarios) varying from 0.3°C to 7.8°C $\Delta TATM$ and from 3% to 99% of near-surface permafrost thawing (Burke et al., 2012; Koven et al., 2013; Lawrence et al., 2012; MacDougall et al., 2012; Mokhov & Eliseev, 2012; Schuur et al., 2013; Slater & Lawrence, 2013). Pooled OLS with two-level clusters by RCP and the Source for heteroskedasticity-robust standard errors is used (the method also implemented by Kessler (2017)). We use Stata and the command `vce()`. The significant results of the regression (from eq. 3) are below in Table 5, wherewith every additional unit of $\Delta TATM$, permafrost thaws by 15.4%.

Table 5. *Regression of Permafrost Thaw.*

	PFthawed
$\Delta TATM$	0.154*** (0.022)
Adj. R ²	0.749
Observations	103

Note. Standard errors in parentheses. ***p < 0.001.

$$PF_{extent}(t) = 1 - \beta \times (TATM(t) - TATM(t_0)) \quad (4)$$

- $PF_{extent}(t)$ is the fraction of permafrost extent at time t

$$C_{PF_{thawed}}(t) = C_{pf} \times (1 - propPassive) \times (PF_{extent}(t-1) - PF_{extent}(t)) \quad (5)$$

- $C_{PF_{thawed}}(t)$ is the carbon in the thawed permafrost at time t (GtC)
- C_{pf} is the total amount of carbon in the near-surface permafrost (GtC)
- $propPassive$ is the share of permafrost in the stagnant pool

⁵ Representative Concentration Pathways (RCPs) are four GHG climate paths (to 2100 and sometimes extended to 2300) used by the IPCC: RCP2.6, RCP4.5, RCP6, and RCP8.5 that correspond to radiative forcing from 2.6 to 8.5 W/m² (van Vuuren et al., 2011).

To obtain projections of the volume of carbon that is made exposed to decomposition by the thawing of permafrost, we need to make hypotheses about the amount of carbon held in the entire permafrost stretch. The following Table 6 shows the most up-to-date assessments of the size of the northern near-surface permafrost carbon pool. Given the closeness of these data assessments, we use the recent one of 1 035 GtC with a 95% uncertainty limit of ± 150 GtC for C_{pf} (1 GtC is a gigaton of carbon that equal to 1 billion tonnes of carbon).

Table 6. *Estimates of Permafrost Carbon Pool (0-3m) (Kessler, 2017).*

Source	Estimate (GtC)	Confidence Interval
(Tarnocai et al., 2009)	1 024	n/a
(Hugelius et al., 2014; Schuur et al., 2015)	1 035 \pm 150	95%

According to Burke et al. (2012, 2013), the size of this stagnant pool is considered ambiguous and could range between 15% and 60% (Table 7).

Table 7. *Estimates of Relative Size of the Stagnant Pool (Kessler, 2017).*

Study	Best estimate (GtC)	Uncertainty range
(Falloon et al., 1998)	n/a	15% - 16%
(Dutta et al., 2006)	18%	n/a
(Burke et al., 2012)	n/a	18% - 60%
(Burke et al., 2013)	n/a	15% - 60%
(Schneider von Deimling et al., 2014)	52.5%	40% - 70%

We take a mid-point estimate of the size of the stagnant pool at 40% for *propPassive* (Burke et al., 2013).

3.1.2. Phase 2: GHG from Permafrost and Infrastructure Damages

This phase, decomposition of carbon in thawed permafrost and carbon dioxide release, is subdivided into 2 parts – GHG release due to permafrost thaw and GHG due to construction activities.

3.1.2.1. CO₂ and CH₄ Due to Permafrost Thaw Model and Data.

Many models of permafrost carbon dissolution are based on a partitioning of vulnerable (melted) permafrost soils into separate carbon pools based on their

breakdown profiles (Burke et al., 2012; Dutta et al., 2006; Elberling et al., 2013; Schädel et al., 2014; Schaefer et al., 2011).

These representations exhibit two main benefits, specifically that they replicate the natural processes at stake and that they do not need a zonation of permafrost soils. However, they also exhibit significant shortcomings. Firstly, there is not sufficient data from field and laboratory experiments to enable us to parameterize the various carbon pools (Schädel et al., 2014). Then, climate change will not only double the amount of carbon that is available for decomposition, but it is also very likely to modify the physical composition and hydrological attributes of permafrost soils (Schuur et al., 2009; Zhuang et al., 2009). Therefore, any characterization of permafrost soils is bound to develop with climate change over the next 300 years. Finally, our choice of description should indicate the level of the ambiguities at stake: we can try dividing the ambiguity on the decay rate into many uncertain parameters and methods, but this conceals the fact that we know little about the rate at which thawed permafrost will disintegrate over the next 300 years. As highlighted by Schneider von Deimling et al. (2014), the extent and timing of carbon fluxes as a result of permafrost degeneration are highly unpredictable.

Ergo, what we recommend here is an uncomplicated procedure, which conceptually fits the notion that the vulnerable carbon can be classified into a slow, fast and stagnant pool; however which does not aim to replicate elaborate and evolving microbial disintegration processes. What we need to evaluate future emissions of permafrost carbon is to understand the intensity at which permafrost carbon will be discharged into the atmosphere, as well as the composition that it will take (CO₂ or CH₄) (Schädel et al., 2014). The approach outlined here relies on subsequent assumptions:

- The passive pool is very stable and not released over the time range of this research, so we focus only on slow and fast pools (Burke et al., 2013)
- The disintegration and discharge of thawed permafrost carbon from those pools can be represented by an exponential decay rate (Schaefer et al., 2011).

Hence, we estimate that the main possibilities about the disintegration phase are the size of the stagnant pool, the rate of disintegration (characterized as the e-folding time) and the proportion of disintegrated carbon that will be discharged as CH₄ or CO₂. Whether permafrost carbon will be discharged to the environment in the form

of carbon dioxide or methane will depend on variations in soil moisture (Natali et al., 2015). Certainly, methane is primarily produced through anaerobic breakdown, which depends on the comparative saturation of the soil (Burke et al., 2012). Given the significant ambivalence surrounding future changes in permafrost soil moisture, and following the procedure generally used in the research (Schneider von Deimling et al., 2014; Schuur et al., 2013), we appropriate that the proportion of methane emissions will remain fixed until 2300. Considering that the disintegration of permafrost carbon ensures an exponential decay function, the volume of thawed permafrost that is discharged at a time (t) in the form CH_4 or CO_2 can be expressed as (6) and (7).

$$CO_{2PFthawed}(t) = CO_{2conv} \times (1 - propCH_4) \times \left(\sum_{s=t_0}^t C_{PFthawed}(s) \times \left(1 - e^{-\frac{t-s}{\tau}}\right) \times \left(e^{-\left(\frac{t-s}{\tau}\right) \times (t-s-1)}\right) \right) \quad (6)$$

$$CH_{4PFthawed}(t) = CH_{4conv} \times (propCH_4) \times \left(\sum_{s=t_0}^t C_{PFthawed}(s) \times \left(1 - e^{-\frac{t-s}{\tau}}\right) \times \left(e^{-\left(\frac{t-s}{\tau}\right) \times (t-s-1)}\right) \right) \quad (7)$$

where:

- $CO_{2PFthawed}(t)$ is the volume of CO_2 in newly thawed permafrost at t
- $CH_{4PFthawed}(t)$ is the volume of CH_4 in newly thawed permafrost at t
- τ is the e-folding time of permafrost disintegration in the active and slow pools (i.e. not in the passive pool)
- CO_{2conv} is the conversion rate from GtC to Gt CO_2
- CH_{4conv} is the conversion rate from GtC to ppb
- $propCH_4$ is the fraction of methane from all GHG
- $C_{PFthawed}(t_0)$ is the carbon (GtC) from thawed permafrost at a time t_0

The disintegration time of the thawed carbon that is not in the stagnant pool is assumed to be in the range of 0-200 years (Burke et al., 2013). We determine an estimate of the parameter τ through existing data assessments of permafrost disintegration rates that are collected in Table 8 below and provided by Kessler (2017).

Table 8. *E-folding of Permafrost Carbon Decomposition (Kessler, 2017).*

Study	e-folding time (years)	Comments
(Dutta et al., 2006)	20	Estimate based on the projection that a 10% thaw of the yedoma stock (46 GtC) would lead to a total of 40 GtC being transferred directly or indirectly to the atmosphere four decades later under a uniform temperature of 5°C.
(Schaefer et al., 2011)	70	Estimate defined as the characteristic e-folding time of permafrost carbon decay.
(Elberling et al., 2013)	34 - 361	Estimate based on a three-pool dynamic model that projects a potential C loss between 13 and 77% for 50 years of incubation at 5°C.
(Knoblauch et al., 2013)	167	Estimate calculated from turnover times of 170.3 years for the stable pool and 0.26 years for the labile pool.
(Schädel et al., 2014)	22 - 224	Estimate based on projections that between 20 and 90% of the organic C will potentially be mineralized to CO ₂ within 50 incubation years at a constant temperature of 5°C.
(Schneider von Deimling et al., 2014)	25 (10 - 40)	Estimate that corresponds to the turnover time of an aerobic slow pool at 5°C.

Based on the assessments, we assume a mean value for the parameter τ of 70 years, which, coupled with the hypothesis that the extent of the stagnant pool stands at c. 40% means 31% of thawed permafrost carbon will have disintegrated after 50 years. This estimation is somewhat below the mean estimates from Elberling et al. (2013) and Schädel et al. (2014) of the portion of total thawed carbon that has disintegrated after 50 years (45% and 55%, respectively). However, their conclusions rely on the premise that the thawed permafrost is exposed to a steady temperature of 5°C, which is why we adjust our estimation slightly less.

There are very few reported estimates of the portion of methane emissions. The only two studies we are aware of which present a precise estimate of the portion of permafrost carbon that will be emitted into the atmosphere as methane are the one

by Schuur et al. (2013), which registers that this proportion will be around 2.3% and the one by Schneider von Deimling et al. (2014), which attests that this proportion will be in the range 1.5% - 3.5%. We appropriate a mean value for the proportion of methane emissions of 2.3%.

3.1.2.2. GHG Due to Construction Activities Model and Data.

Construction and upkeep of infrastructure release a significant amount of GHG into the atmosphere, which most of the climate models accurately capture. Also, as discussed in previous sections, there has been a significant increase in infrastructure in the Arctic region. These infrastructures are at severe risks due to permafrost thaws. Although due to advancement in research and engineering techniques, the infrastructures built on permafrost are more stable than ever, this stability also has a limit, which depends on thawing activity. Beyond a certain level of thaw, most of the infrastructure would undergo severe deformation. Resulting in partial or complete loss of the building. Consequently, these damages would have to be recouped both in terms of managing the waste generated from the damages and rebuilding of infrastructure. Both of these activities generate the same level of GHG emissions as routine construction activity. Permafrost thaw itself is a ticking carbon time bomb, which researchers and scientists have started incorporating into the climate models in recent decades. But the carbon release potential due to infrastructure damage is often overlooked. Hence, we incorporate the infrastructure damages due to permafrost thaw along with normal thaw into the DICE 2016 model.

This section has two subdivisions; where first, we estimate the area of infrastructure that is at risk due to permafrost thaw. Second, we calculate the potential carbon release from damage and reconstruction of infrastructure.

3.1.2.2.1. Estimating Infrastructure at Risk due to Permafrost Thaw

The steps to estimate the area of infrastructure at risk due to permafrost thaw:

- a) Ingesting Permafrost data
- b) Uploading the three datasets into code editor:
 - 1) Permafrost extent, 2) Settlement grid, 3) Night-time light.
- c) Extracting images from feature collection and image collection
- d) Filtering the images into required bands for processing
- e) Masking (overlapping) the permafrost image with settlement image
- f) Calculating the area of the resultant image for different attributes
- g) Cross verification by masking the resultant image with a night-time light and recalculating the area.

As there are no data on the presence or absence of permafrost under an infrastructure, we use separate data of settlement and permafrost extent and night-time light emission to estimate it.

The data used are of two types: historical temperature data and the current permafrost spread and habitation on permafrost in the form of GIS file format. The historical temperature data is used to calculate the total area that would be affected by climate change and the resulting carbon release. GIS data is used to calculate the total area of infrastructure that is on top of active permafrost and at risk from the thaw. The GIS data is taken from Google Earth Engine dataset, NASA, Earth Observation Group and US Air Force (Elvidge et al., 1999, 2013, 2017; Hsu et al., 2015; National Snow and Ice Data Center, n.d.; Pesaresi & Freire, 2016; Sato & Schmidt, n.d.)

Regarding the first-part data for permafrost extent, we use the data from National Snow and Ice Data (Heginbottom et al., 2002). The NSIDC advances study into our world's cryosphere. The circumpolar permafrost and ground ice data provide a unified international data set representing permafrost and ground ice's properties and distribution in the Northern Hemisphere (20°N to 90°N). The re-gridded data set shows continuous, discontinuous, sporadic, or isolated permafrost boundaries. Permafrost extent is calculated in percentage area (90-100%, 50-90%, 10-50%, less than 10%, and 0%). The corresponding abundance of ground ice in the upper 20 m is calculated in percentage volume (greater than 20%, 10-20%, less than 10%, and no permafrost). The data set also comprises the position of subsea and relict permafrost. The gridded data are gridded at 12.5 km, 25 km, and 0.5-degree resolution. The shapefiles are acquired from the original 1:10 000 000 paper map (Brown et al., 1997).

The data for the second part, global settlement extent, is taken from the Google Earth Engine data catalogue (*Earth Engine Data Catalog | Google Developers*, n.d.). Earth Engine's public data catalogue encompasses a mixture of standard Earth science raster datasets. The dataset is termed GHSL: Global Human Settlement Layers, Settlement Grid 1975-1990-2000-2014. The GHSL relies on devising and executing innovative spatial data mining technique to automatically prepare and extract insights from a vast amount of heterogeneous data. The source includes global, fine-scale satellite image data streams, census data, crowdsourcing, or volunteered geographic information sources. Every grid in the GHS-SMOD has been created by blending the GHSL built-up areas and GHSL population grids data

for reference epochs: 1975, 1990, 2000, 2015. The DEGURBA (Degree of Urbanization) classification schema is a people-based representation of towns, cities and settlements: it operates using as principal input a one km² grid cell estimating for the population at an epoch. The DEGURBA divides the population grid cells into three main categories: 'urban centres' (cities), 'urban clusters' (towns and suburbs), and 'rural grid cells' (villages and others). These class concepts translate to 'high-density clusters (HDC)', 'low-density clusters (LDC)', and 'rural grid cells (RUR)' sequentially in the GHS-SMOD dataset. In the dataset, the 'HDC' is the spatial generalization of contiguous population grid cells (4-connectivity, gap-filling) with a density of at least 1500 inhabitants per km² or a built-up surface density > 50%, and a minimum total resident population of 50 000. The 'LDC' are consecutive grid cells with a frequency of at least 300 inhabitants per km² and a total population of 5000 or more. The 'RUR' are grid cells other than 'HDC' and 'LDC' with a population of more than 0 and less than 300. Everything else is listed as inhabited areas where the population is equal to 0. The Global Human Settlement Layer (GHSL) project is sponsored by the European Commission, Joint Research Center, and Directorate-General for Regional and Urban Policy.

The Google Earth Engine database provides the third part of data night-time. The dataset is called Global Radiance-Calibrated Night-time Lights Version 4, Defense Meteorological Program Operational Linescan System. NOAA's National Geophysical Data Center does image and data processing of the dataset, and US Air Force Weather Agency collects the data. The Defence Meteorological Program (DMSP) Operational Line-Scan System (OLS) has a novel ability to distinguish visible and near-infrared (VNIR) emission origins at night. This compilation comprises global night-time lights images with no sensor saturation. The sensor is usually operated at a high gain setting to facilitate the detection of moonlit clouds. However, with six-bit quantization and a short dynamic range, the recorded data are concentrated in urban centres' bright cores. A bounded set of observations at low lunar illumination were taken where the detector's gain was set significantly lower than its typical operational setting (sometimes by a factor of 100). Sparse data collected at low-gain settings were merged with the operational data collected at high-gain settings to create the set of global night-time lights images with no sensor saturation. Data from several satellites were synthesized and blended into the final product in order to obtain maximum coverage.

All the above datasets are pan-global and are available for free public use. After gathering all the relevant data, the next step is to analyse the data. As mentioned before, the magnitude of the data is so vast that personal computers would not be able to process it efficiently. Therefore, we use Google Earth Engine to process this data. Google Earth Engine consolidates a multi-petabyte catalogue of satellite imagery and geospatial datasets with planetary-scale analysis abilities. GEE makes it available for researchers, scientists, and developers to distinguish changes, map trends, and quantify variations on the Earth's surface. Earth Engine is a program for scientific analysis and visualization of geospatial datasets for government, academic, non-profit, business and average users. Earth Engine hosts satellite imagery and repositories in a public data archive that incorporates historical earth images dating back more than forty years. The images, ingested daily, are then made ready for global-scale data mining.

After ingesting the dataset into GEE, we analyse the dataset and the various attributes associated with it.

Table 9. *Permafrost Extent Attributes.*

No	Attributes	Values	No of Observations
1	Ground ice content	Low	3699
1	Ground ice content	High	396
1	Ground ice content	Medium	273
2	Permafrost extent	Continuous (90-100%)	2411
2	Permafrost extent	Glacier	2226
2	Permafrost extent	Discontinuous (50-90%)	781
2	Permafrost extent	Isolated Patches (0-10%)	609
2	Permafrost extent	Sporadic (10-50%)	567

The unit of observation in Table 9 is a strip of a map that can vary in area. The Ground ice content classifies how thick the ice is below the permafrost, and the Permafrost extent classifies what kind of permafrost spread it is.

Figure 2. *Permafrost Extent Layer Image.*



Note. Made by the authors, coding in Google Earth Engine (*Google Earth Engine*, n.d.) and using data source (National Snow and Ice Data Center, n.d.).

In Figure 2 above, the permafrost extent is represented. The lightest shade of blue represents the continuous permafrost. The medium-dark blue shows the discontinuous permafrost on the map. Lastly, the darkest blue notes both the sporadic and isolated permafrost.

Table 10. *Settlement Extent.*

No	smod_code	Description
1	0	Inhabited areas
2	1	RUR (rural grid cells)
3	2	LDC (low-density clusters)
4	3	HDC (high-density clusters)

The attribute of importance in Table 10 is the Degree of urbanisation, which is referred to as smod_code. The various values in that code are shown. For our analysis, we take all the infrastructure above value 0. In that way, we focus on the infrastructure in rural, low density urban and urban area.

Figure 3. *Settlement Layer Image (Partial).*

Note. Made by the authors, coding in Google Earth Engine (*Google Earth Engine*, n.d.) and using data source (Pesaresi & Freire, 2016).

In Figure 3 above, we show Europe only in order to show different intensities of settlement, whereas the calculations are done on the global level further in the paper. The settlement layer shows the intensity of infrastructure, ranging with white as the highest intensity, dark brown as the lowest, and shades of blue in between. The lighter colour indicates a higher value of the settlement, meaning that the infrastructure there is more advanced. We can see on the map that the largest cities such as London, Paris and Milan are in white. The area surrounding the cities are in lighter blue. The coastlines are also covered in higher-intensity settlement, indicated by the lighter shade of blue.

Table 11. *Night-time Light.*

No	Name	Min	Max	Description
1	avg_vis	0	6060	Average digital band numbers from observations with cloud-free light detection.

The parameter of interest here is the average illumination of night light (Table 11). This parameter is represented by avg_vis. The range of value is from 0 to 6060.

Figure 4. *Night-light Layer Image (Partial).*



Note. Made by the authors, coding in Google Earth Engine (*Google Earth Engine*, n.d.) and using data sources (Elvidge et al., 1999, 2013, 2017; Hsu et al., 2015).

In Figure 4 above, Europe is also portrayed again. The night-light layer shows the intensity of light during the night. The clusters of the white colour show the largest and most active cities on the map. That corresponds to the settlement image, where the largest cities such as London, Paris and Milan have the highest night light intensity, confirming the settlement data layer.

The datasets contain collection images and features. To combine two datasets, we initially need to extract image from the image collection and feature collection. Therefore, we extract the image from the permafrost feature collection using the attributes of ground ice content and permafrost extent. Similarly, we extract image from the image collection of settlement extent using a degree of urbanisation. After generating the two images, we mask the image of permafrost extent, with different ground ice content and permafrost extent values, with the image of settlement.

The next step is to calculate the area of the overlapping regions of two images. To calculate the area, we use the resolution of a dataset of permafrost extent. Then, using the resolution, we calculate the area of the masked pixel, and then we multiply it with the total number of pixels in the masked image. After calculating the area of different permafrost extent, we validate it using the night-time data. The idea behind using this dataset is that if there is settlement present, then, most likely, there will be some sort of light present during the night in the same area. Hence, we extract the image from the image collection of the night-time light dataset using the average

luminance value. Afterwards, we follow the same process as above, but instead of using the settlement image, we use the night-time light image to mask the permafrost image.

After estimating the individual area of infrastructure on different types of permafrost spread, we recombine the area to calculate the total affected area. To combine the values, we use the approach used by Porfiriev et al. (2019).

In a general form, the calculation formula is the following:

$$A = 0.9Ac + 0.05Ad + 0.1Af \quad (8)$$

where A is the total area of infrastructure built on permafrost, Ac is the area of infrastructure built in the zone of continuous permafrost, Ad is the area of infrastructure built in the zone of discontinuous permafrost; Af is the area of infrastructure built in the zone of massive-island (fragmentary) permafrost.

3.1.2.2.2. Carbon from Infrastructure Damage and Reconstruction

After calculating the total area of infrastructure at risk, the next task is to convert it into potential carbon emissions. Since it is difficult to calculate the exact dimension, building material or building process associated with each building or infrastructure, we adopt a generalised approach to estimate the carbon emission from infrastructure damage and reconstruction. Hong et al. (2015) calculates the greenhouse gas emission during various phases of construction and gives out a general estimate for the amount of CO₂ released per square meter both during the construction phase and during the lifecycle of the infrastructure. The estimates from the paper gave the carbon emissions intensity as 0.38 tCO₂e/m² Yr during the construction process and 0.06 tCO₂e/m² Yr during the building usage stage. The construction phase lasted 2 years, and building usage 50 years. Therefore, the total carbon emissions during the construction phase are 0.76 tCO₂e/m² and 3 tCO₂e/m² during the usage phase of the building. As mentioned before, when the infrastructure is damaged due to permafrost thaw, we have to reconstruct the building, and at the same time, the emission from lifetime usage of the building is emitted out at once. Hence, the emission from per square meter of damage would cause (3 + 0.76) tCO₂e/m² of emission.

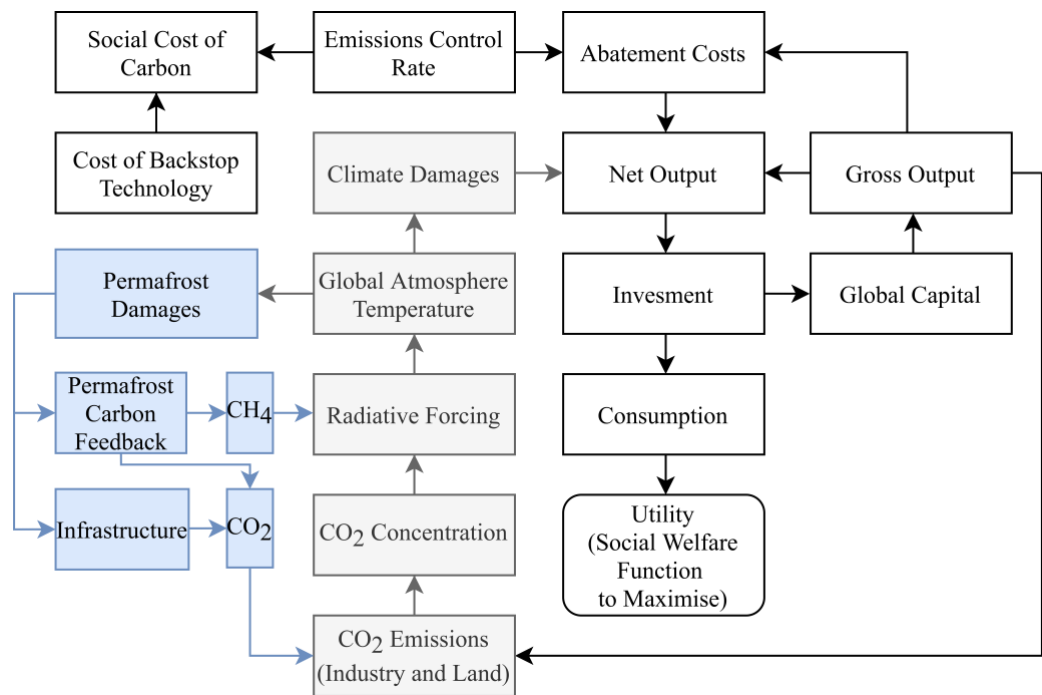
These 2 subparts of phase 2 give near holistic carbon feedback due to permafrost thaw. Now to calculate the economic impact of this carbon feedback, we decided

to use the DICE⁶ model as the framework for our analysis of the impacts of the PCF, as it is one of the most well-known IAMs and one which has often been used to provide estimates of the SCC.

3.1.3. Adding Permafrost and Infrastructure GHG to DICE-2016R

We incorporate our estimated part of the permafrost carbon feedback and infrastructure rebuilding emissions into the DICE-2016R⁷ optimisation model. Figure 5 shows the simplified representation of DICE. The climate elements are represented in grey, economic in white. Then, we add the permafrost and infrastructure damage module (in blue) to the original optimisation problem.

Figure 5. DICE Model Simplified Representation.



Note. The scheme is modified by authors (DICE Model Background, n.d.; Kessler, 2017).

We use Python and the translated code proposed by Krichene (2019). The optimisation maximises the social welfare function (Nordhaus, 2017b):

$$W = \sum_{t=1}^{Tmax} U[c(t)L(t)R(t), \tag{9}$$

⁶ For the description of revised DICE-2016R model and references to all equations and models, see (Nordhaus, 2017b).

⁷ We define the modified or additional equations in this paper, but for all the list of equations in the Python code, please refer to Nordhaus (*DICE/RICE Models - William Nordhaus | Yale Economics*, 2020).

Where U is the utility function, $c(t)$ is consumption, $L(t)$ is population, $R(t) = (1 + \rho)^{-t}$, being a sensitive point as explained in Equation (2). The function of utility has α - generational inequality aversion/elasticity of the marginal utility of consumption (as the marginal utility elasticity η in Equation (2)) and has the form $U(c) = \frac{c^{1-\alpha}}{1-\alpha}$.

The permafrost carbon feedback contributes to the CO₂ and CH₄ emissions that influence the radiative forcing and the global mean temperature. Global temperature change is the key variable in estimating climate damages in monetary terms in a quadratic function. According to Nordhaus (*DICE/RICE Models - William Nordhaus / Yale Economics*, 2020; 2017b), the damage is $\Omega(t) = \frac{D(t)}{1+D(t)}$ and

$$D(t) = \varphi_1 TATM(t) + \varphi_2 (TATM(t))^2 \tag{10}$$

- $\varphi_1 = 0$ (intercept is zero)
- $\varphi_2 = 0.00236$

Moreover, the radiative forcing parameters from non-CO₂ GHG in original DICE are set as approximate values of 0.5 in 2015 and 1 in 2100 and based on the RCP 6.0W/m² (*DICE/RICE Models - William Nordhaus / Yale Economics*, 2020; Nordhaus & Sztorc, 2013). Instead, we estimate more precise values for the non-CO₂ GHG radiative forcing (with and without permafrost and infrastructure feedback) using the formulae (Table 12 below) presented in the Fifth Assessment Report of the Intergovernmental Panel on Climate Change by Myhre (2013). We take data from NASA comprising methane (CH₄) and nitrous oxide (N₂O) expressed in ppb (parts per billion) for RCP 6.0W/m² (Sato & Schmidt, n.d.). The methane from permafrost is also added to the calculations in the model when PCF is taken into account.

Table 12. *Formulae for Radiative Forcing (RF) from CH₄ and N₂O.*

Gas	RF (W/m ²)	Constant α
CH ₄	$\Delta F = \alpha(\sqrt{M} - \sqrt{M_0}) - (f(M, N_0) - f(M_0, N_0))$	0.036
N ₂ O	$\Delta F = \alpha(\sqrt{N} - \sqrt{N_0}) - (f(M_0, N) - f(M_0, N_0))$	0.12

Note. $F(M, N) = 0.47 \ln[1 + 2.01 \times 10^{-5} (MN)^{0.75} + 5.31 \times 10^{-15} M(MN)^{1.52}]$, M is CH₄ in ppb, N is N₂O in ppb. The subscript 0 denotes the unperturbed molar fraction for the species being evaluated. However, note that for the CH₄ forcing, N₀ should refer to present-day N₂O and for the N₂O forcing, M₀ should refer to present CH₄.

4. Results and Discussion

4.1. Permafrost and Infrastructure Effects

In this section, we present and discuss the environmental and economic effects caused by the permafrost carbon feedback and the infrastructure damages. First, we present the emissions from infrastructure and permafrost. Second, we compare the output of our optimisation model with the original optimal DICE-2016R model. Both models have the altered radiative forcing formula. The comparison is followed by the discussion that also includes the work from various authors estimating the effects of permafrost feedback to check the validity of our results compared to similar research.

4.1.1. Infrastructure Carbon Emissions

Using the steps and layers discussed in the methodology, the following results of masked images of permafrost and settlement are shown below. To make the visualization clearer, we present different layers and a masked result for a smaller Yakutsk area, whereas the calculations are made on the global level. The colours used are the same as in the methods section.

In Figure 6 below, we can see the permafrost layer. The light blue colour is overlapping with almost the whole map, indicating that the area is on continuous permafrost. The settlement layer (Figure 7 below) shows the light blue shade and white colour for the highest intensity for infrastructure, verified by the night-light layer (Figure 8) white colour of the highest light intensity in the centre of Yakutsk.

Therefore, we get masked – all layers result in Figure 9, where the settlement, night-light and permafrost areas overlap. That gives higher accuracy of the actual area that is with infrastructure and in the risk of permafrost thaw.

Figure 6. Permafrost Layer.

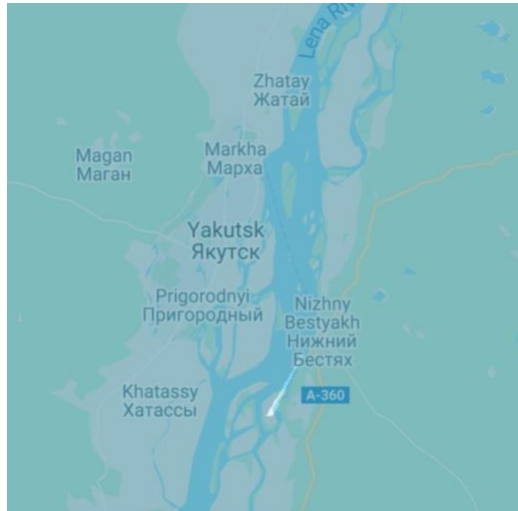


Figure 7. Settlement Layer.

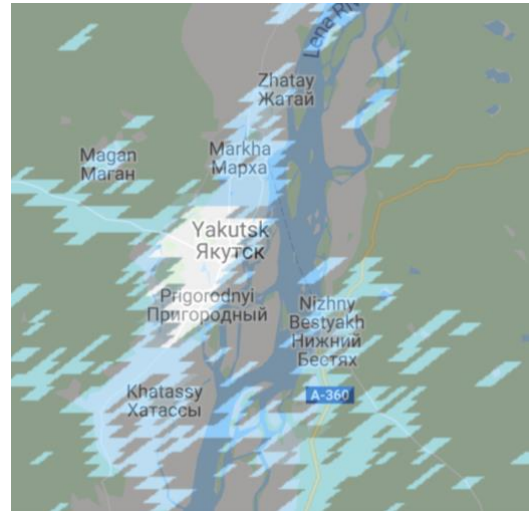


Figure 8. Night-light Layer.

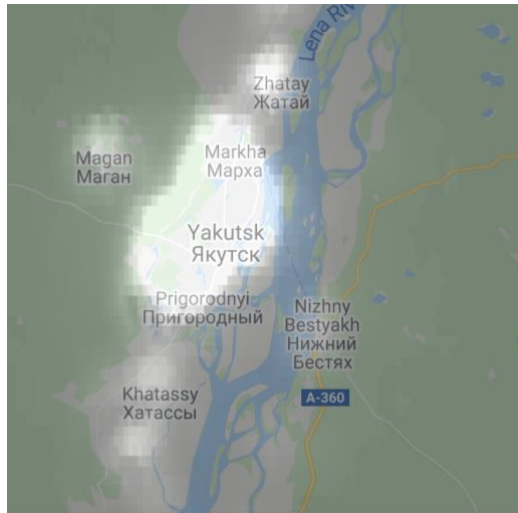


Figure 9. Masked - All Layers.



The comparison between the areas of infrastructure on top of permafrost is shown below in Table 13. The two areas are calculated from permafrost image collection masked with settlement and nightlight dataset, respectively. The data is at the global level.

Table 13. Masked Area for Settlement and Nigh-time light.

No	Infrastructure on different permafrost spread	Masked area with Settlement index (km ²)	Masked area with Night-time light (km ²)
1	Continuous	426	404
2	Discontinuous	1760	1667
3	Isolated Patches	5833	5685
4	Sporadic	2059	1723

From Table 13, we can see that area of the mask calculated using both settlement and night-time light has higher accuracy than only using settlement index. The higher accuracy is the result of different spatial resolution of both the dataset. Therefore, we use a combination of both.

Using the same principle by combining the areas of infrastructure on different types of permafrost using the same ratio. The calculations are shown below.

$$\begin{aligned}
 A &= 0.9Ac + 0.5Ad + 0.1Af \\
 &= 0.9 \times 404 + 0.5 \times 1667 + 0.1 \times (5685 + 1723) \\
 &= 1037.9 \text{ km}^2 \text{ or } 1937 \times 10^6 \text{ m}^2
 \end{aligned}
 \tag{11}$$

From the above calculations, we have the total area at risk ($1937 \times 10^6 \text{ m}^2$). The calculations using the above values of carbon release are shown below to estimate the total CO₂ release from infrastructure damage due to permafrost thaw (multiplying the area at risk and carbon emissions per m^2 of construction).

$$1937 \times 10^6 \text{ m}^2 \times (0.76 + 3) \frac{\text{tCO}_2\text{e}}{\text{m}^2} = 7.283 \text{ GtC}
 \tag{12}$$

4.1.2. Permafrost Carbon Emissions

Figure 10. *Permafrost Extent.*

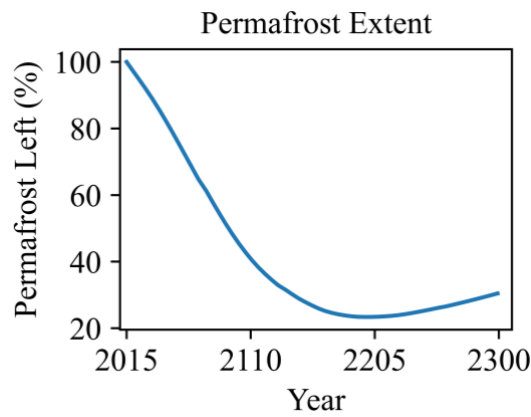
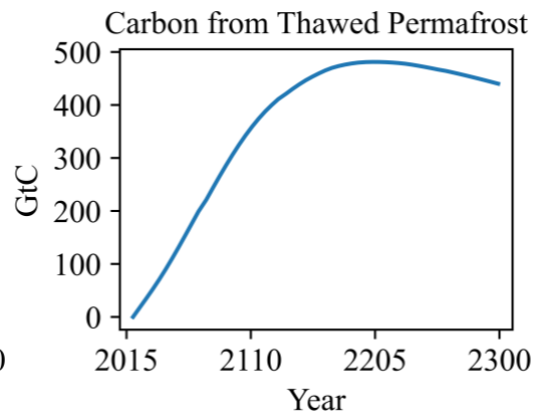


Figure 11. *Carbon from Permafrost.*



Stemming from Equations (4) and (5) that we integrated into the DICE-2016R, the permafrost extent, which depends on the temperature of the atmosphere and is measured as a percentage of the initial permafrost area, decreases. It reaches 36% in 2121 and the lowest point of 23% in 2198 (Figure 10), which is a little bit less than the predictions that 65% will thaw, leaving 35% by around 2100 and decline further (Kleinen & Brovkin, 2018). After the lowest point, the permafrost extent gradually increases since it can refreeze (Schneider von Deimling et al., 2012).

However, due to the e-folding time of carbon decomposition, the GHG can be still released by the permafrost that thawed in the past. Regarding the cumulative carbon from permafrost in Figure 11, it reaches 325 GtC by 2100. This is in the bound of 140-400 GtC by the end of the century stated by Nitzbon (2020), and 68-508 GtC by 2100 claimed by MacDougall (2012). By 2300, it reaches 440 GtC, which is predicted in the bounds 381–616 GtC (RCP 8.5 scenario) by Schuur (2013). The evaluations comprise both CO₂ and CH₄. Therefore, as per our aforementioned results and discussion, the cumulative carbon emissions are on a higher side of the estimations provided by the researchers but still consistent with the literature.

4.1.3. Combined Environmental Impact

Figure 12. Radiative Forcing.

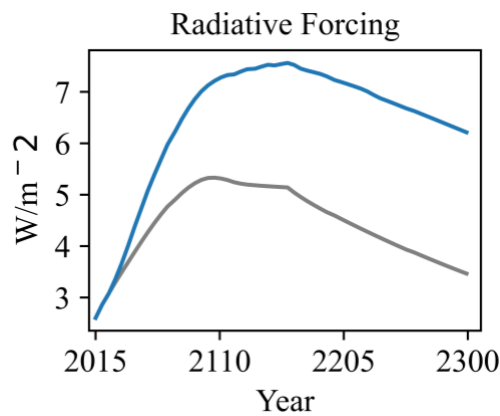


Figure 13. Emissions.

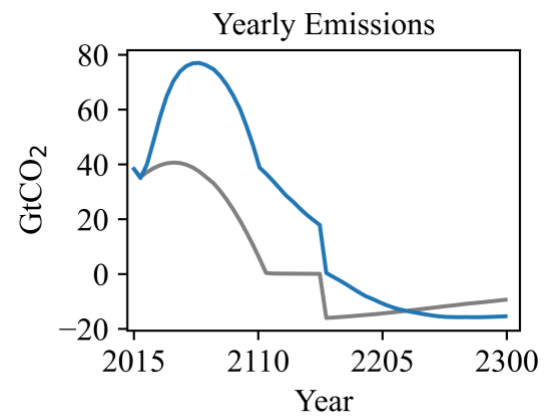


Figure 14. TATM.

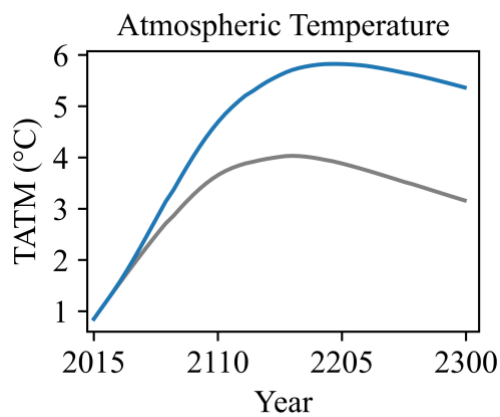
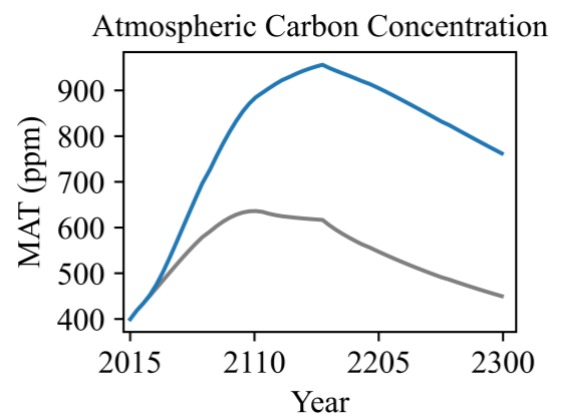


Figure 15. MAT.



Observing the environmental impact of the permafrost and infrastructure damage emissions, we see an increase in the overall radiative forcing in Figure 12 and yearly emissions in Figure 13 (original-altered forcing model in grey, with permafrost and infrastructure added module in blue). The carbon feedback pushes the forcing towards the worst-case RCP8.5 scenario, which is similar to the business-as-usual scenario and not optimal (Michaelis & Wirths, 2020; Nordhaus, 2018). The emissions in Figure 13 increase much higher due to permafrost thaw and infrastructure damages, but also reaches 0 and goes negative. This is due to the fact that DICE assumes the possibility of removing carbon from the atmosphere using the backstop technology. In the DICE model, a backstop technology is either carbon-neutral, replaces fossil fuels or removes carbon emissions (Nordhaus & Sztorc, 2013). However, there are no current studies that use DICE-2016R and permafrost to compare the radiative forcing and yearly emissions. Due to this reason, we concentrate on the atmospheric temperature and carbon concentration that are interrelated with radiative forcing and yearly emissions and where research results are more abundant.

As we can see in Figure 14, the atmospheric temperature (TATM) is much higher compared to the original model. Firstly, there is no difference in temperature for the first 25 years. Secondly, in the original model (grey), the temperature flattens out around 2110 under 4°C, whereas the temperature in the model with permafrost and infrastructure keeps increasing until 2200 to the maximum point of 5.8°C. The reason for these two observations stems from the e-folding time or exponential decay. Since the permafrost thaw releases the GHG gradually over time, it keeps increasing even though the temperature stopped causing the thaw. The permafrost and infrastructure module leads to an additional temperature increase of 2.2°C at the end of 2300. This is a very high additional increase, higher than the worst-case scenario bounds of 0.13 – 1.69°C by 2300 provided by MacDougall et al. (2012). Though, it is important to state that their article did not simulate methanogenesis, and all emissions were assumed to be CO₂. As we include methane in our research, it is claimed that it could contribute to an additional 0.12 - 0.5°C in 2300 (Parker, 2016). Moreover, we also have an additional element of infrastructure damage emissions. In that way, our temperature finding is at the higher bound and is valid.

Figure 15 shows the atmospheric carbon concentrations in ppm (parts per million). Here we also witness that the carbon concentration keeps significantly increasing for the permafrost and infrastructure model, while the original model is

relatively stable around 2100-2150. The reason is also related to the delayed permafrost thaw carbon decomposition and the e-folding. Even if we stopped permafrost from thawing at a one-time point, the carbon concentration would still be released. That can also be the cause of ‘tipping points’, when damage is irreversible. The additional ppm from permafrost and infrastructure adds 312 ppm compared to the optimal original-altered forcing case at the end of the 23rd century. MacDougall et al. (2012) found that the net contribution of permafrost could be in the range of 82–338 ppm (scenario 6.0) or 196–374 ppm (scenario 8.5), so our findings are congruent with the authors. The relation between temperature and concentration of carbon differs from MacDougall et al. (2012) due to the fact that they use the University of Victoria (UVic) Earth System Climate Model (ESCM), whereas we use a different and simplified DICE model, where the emissions depend primarily on temperature. Thus, as our results and discussion tell, the environmental impact of permafrost carbon feedback and infrastructure damage rebuilding emissions is similar to the usually highest bound or predictions by previous research. It is crucial to add additional damages to calculate the effects and be alarmed about the irreversible effects it can add to the temperature and carbon concentration increase.

4.1.4. Combined Economic Impact

Figure 16. Damages.

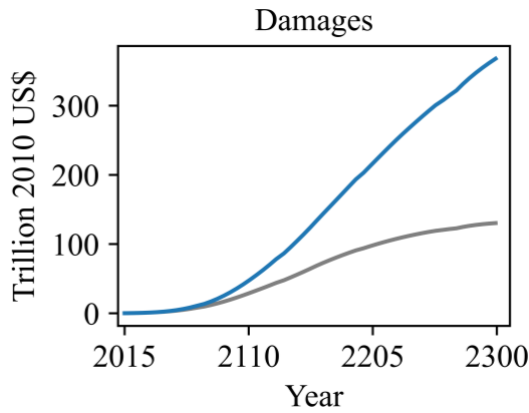


Figure 17. Control Rate.

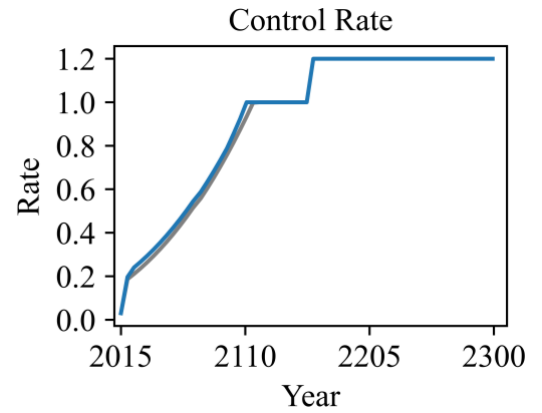


Figure 18. Investment.

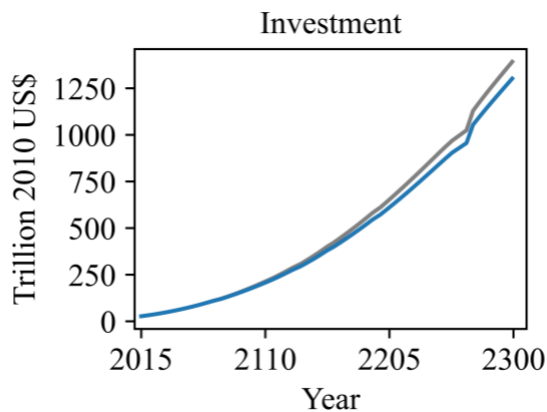
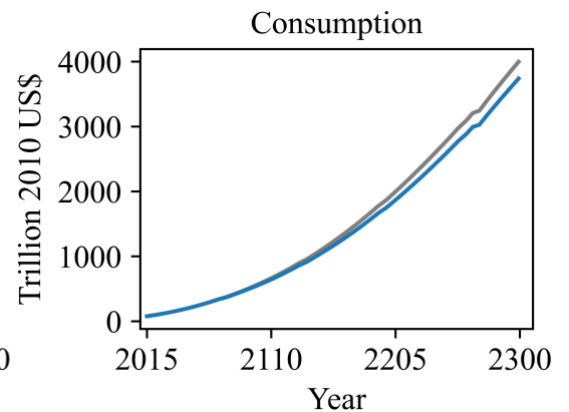


Figure 19. Consumption.



As per Figure 16, we see no difference in climate damages in the first 50 years since the permafrost again releases the carbon gradually due to e-folding time. Also, it takes some time for policymakers to react and abate the cost, delaying the effect on losses. After that, the climate damages skyrocket. The additional climate damages (Equation 10 in method section) due to permafrost and infrastructure (blue) compared to the original-optimized forcing optimal model (grey), reach 110 trillion US dollars by 2200, which is in range with results of 3 – 166 trillion dollars by Hope and Schaefer (2016). The results are again on the higher side of the bounds, which is explainable due to the additional infrastructure element. However, it is much higher than the predicted 70 trillion dollars by later research using a different model PAGE-ICE (Yumashev et al., 2019). The lack of DICE-2016R model usage by other researchers can result in such discrepancies between models.

In Figure 18 and 19, the investment and consumption are presented, respectively. With the permafrost feedback and infrastructure damages (blue), both investment and consumption decrease by approximately 7% by 2300. Therefore, the output also decreases since it is the sum of consumption and investment (Nordhaus & Sztorc, 2013). The proportional size of investment and consumption decline due to permafrost and infrastructure seems much lower than the effect on damages, temperature or carbon concentration proportional increase. This is since the output consists of capital, labour and energy, and the climate damages are a smaller but significant share of the total world output. In the neoclassical growth model (Ramsey model), we make investments to lower the consumption now so we can consume more in future (Nordhaus, 2017b). The emissions from thawing permafrost and also from infrastructure rebuilding lower the levels that the society can invest now and consume in future since higher mitigation costs, together with a higher control rate (Figure 17) coming from the strength of mitigation policies, are needed to prevent from climate change damages. Irreversible damages would make decarbonization efforts ineffective. Permafrost carbon feedback and infrastructure damages make the future damages higher, and the reductions of emissions must start now to evade the future constraints. It is stated that the reductions have to start 20-30 years before gaining the benefits (Kolev et al., 2012). Consequently, it is important to switch to new technologies as early as possible to enhance the welfare that stems from innovation, economies of scale, spillover effects and increased productivity that all lead to long-term growth (Kolev et al., 2012). Climate damage costs significantly increase if we take permafrost carbon feedback and infrastructure damages. It is the call for the nesses to switch to green technologies as early as possible and governments to support them. In the DICE model, the price of backstop technology starts high and decreases over time due to technological advancements (Nordhaus & Sztorc, 2013).

In order to incentivize companies to invest in clean technologies using carbon price, it has to be high enough, so the backstop price is economically viable to invest in green technologies. In the model, the social cost of carbon is the lower value out of the current carbon price or the backstop technology price. The social cost of carbon is also commonly known as a carbon price, so we use it interchangeably.

Figure 20. Carbon Price in 2010US\$.

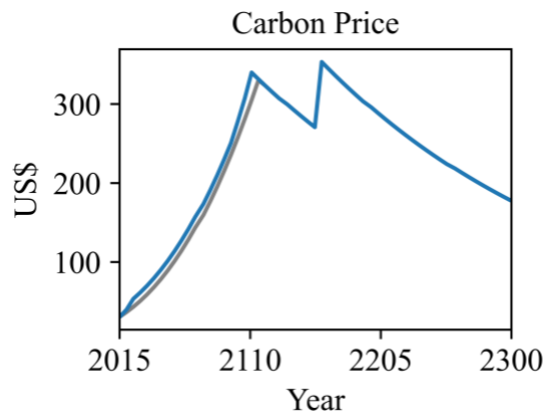
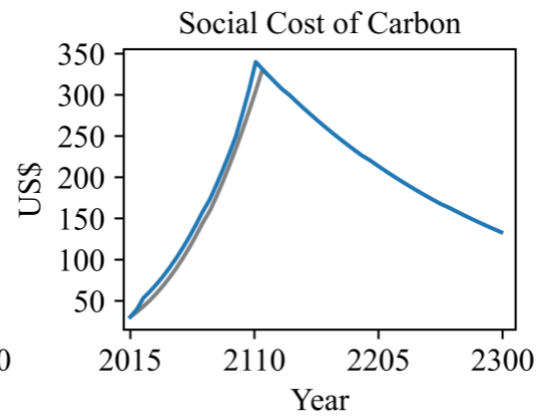


Figure 21. SCC in 2010US\$.



As per Figure 20 and 21, due to higher emissions control rates, the carbon price and social cost of carbon are higher when we include the permafrost and infrastructure (blue) into the DICE-2016R model. The absolute maximum amount of SCC with permafrost and infrastructure is 339.97\$ in the year 2111, which is 11.5% higher than the SCC optimal for the global social welfare function.

Table 14. Social Cost of Carbon DICE-2016R (2010 US\$).

Optimal Scenario	2015	2020	2025	2030	2050
Original (Nordhaus, 2017b)	29.5	35.3	41.8	49.2	99.6
Original - Altered Forcing	30.4	36.5	43.2	50.7	89.2
PF&I	30.4	39.7	53.5	61.4	101.5

As described in the methods section, we changed the module of radiative forcing of other GHG to make it more precise in our analysis. As a result, we have different values in the Original – Altered Forcing model compared to the Original (Nordhaus, 2017b) (Table 14). The SCC is a little higher at the beginning and lower than predicted in 2050 since the calculated radiative forcing using NASA data does not reach the approximate level defined by Nordhaus. Throughout our work, we compare the Original - Altered Forcing model to PF&I, where we add permafrost and infrastructure emissions (Table 14).

In Table 14, the SCC increases by 23.84% in 2025, 21.10% in 2030 and 13.79% in 2050. Overall, the SCC due to permafrost and infrastructure emissions increases between 6-24% (rounded) until 2100. The relative costs related to permafrost and infrastructure are higher in the beginning in order to tackle present damages and avoid greater damages in the future. The results are consistent with, but a little bit higher for the upper bound, Kessler (2017), where she states that the permafrost

carbon feedback increases the SCC by 10-20% using an earlier version of DICE-2013R and with González-Eguino and Neumann (2016), where they estimated the carbon costs and mitigation 6–21 % higher due to permafrost. The higher upper bound is due to infrastructure emissions due to permafrost damages that are under-researched. Therefore, the findings support the argument that the SCC is underestimated in the IAMs.

4.2. Sensitivity Analysis of SCC for 2025

To check the robustness of the SCC results, we conduct a sensitivity analysis in this section that includes altering the critical parameters in the model that are backstop price (a key point in defining SCC and can impact mitigation costs (González-Eguino & Neumann, 2016)) and the elasticity of marginal utility (η) (Equation 2).

Table 15. *SCC 2025 (2010 US\$) Sensitivity Analysis.*

Backstop technology (2010 US\$)	Scenario	The elasticity of marginal utility (η)		
		1.05	1.45	1.85
440	Original - Altered Forcing	73.4	42.9	26.9
	PF&I	73.6	43.3	27.3
	Change	0.3%	0.9%	1.5%
550	Original - Altered Forcing	73.4	43.2	27.0
	PF&I	91.8	53.5	34.1
	Change	25.1%	23.8%	26.3%
660	Original - Altered Forcing	75.0	43.4	27.1
	PF&I	110.2	64.1	40.4
	Change	46.9%	47.7%	49.1%

The DICE-2016R uses the calibrated value of 1.45 for the elasticity of marginal utility (η), which is the estimate of the utility change with an additional unity of consumption, and it is one of the key factors for the SCC (Asplund, 2017; Heal & Millner, 2014). Then, DICE uses 550 2010US\$ as an initial backstop price, declining by 2.5% per period (Nordhaus, 2017b; Nordhaus & Sztorc, 2013). We take the SCC for 2025, where the difference to the Original – Altered Forcing model is the highest due to serious initial damages and control.

As anticipated, Table 15 shows that the SCC increases for lower values of elasticity of marginal utility (η) (lowering the discount rate in Equation 2) and for

higher costs of backstop technology. With the potential impact of permafrost and infrastructure, the difference in SCC drastically changes with the increase of backstop technology price in 2025. The price change varies from 0.9% to 47.7% due to permafrost and infrastructure emissions for the initial backstop technology price from 440 to 660 (2010 US\$) in 2025. This means that if the backstop technology is relatively affordable or supported by governments, it is advantageous for companies to tackle the initial climate damage risks with cleaner energy as soon as possible in order to avoid climate damages and losses in future due to permafrost infrastructure and proliferating mitigation costs that are reflected in carbon prices in future, that are currently underestimated but are rising dramatically.

4.3. Implications of SCC for Businesses

Business analytics evaluate the potential effect of future carbon prices on important financial ratios and competitiveness. Climate expenditure today resembles an insurance policy to reduce the risk of future climate catastrophes, translating the risk into a higher carbon price (Stern & Stiglitz, 2021). As per our analysis, thawing permafrost has a global impact even though it covers only 11% of the Earth's surface (Obu, 2021). Business leaders globally should keep in mind that the SCC is underestimated due to permafrost and infrastructure emissions while making decisions. Permafrost and infrastructure climate damages prove that the social cost of carbon has to be much higher in company evaluations and IAMs to shift to greener investments and tackle the damages in future and shifting would make a positive impact reducing the emissions and also future mitigation resources and costs. Sensitivity analysis also shows that the decisions should be made earlier since that would be effective in 2025, and companies should seek opportunities and government support.

Nevertheless, the climate analytics adopted in companies is a relatively new but emerging concept and collaboration between business, and climate science is needed (Fiedler et al., 2021). The business community should be aware that climate analytics and data should not be misused by putting too much trust in the estimations that are not adapted to the business needs, leading to abuse of science. Therefore, Fiedler et al. (2021) encourage businesses to consider climate translators who would be bridging the gap between complex climate models and non-experts in climate. Climate analytics in the companies should be implemented cautiously and carefully in order to not under- or over-estimate the risks.

5. Conclusion

This thesis studies the combined impact of permafrost carbon feedback and infrastructure reconstruction emissions due to permafrost thaw on the Social Cost of Carbon in the DICE-2016R model, which maximises the social welfare function. The impact stems from the fact that permafrost carbon feedback negatively affects climate by releasing carbon and damaging infrastructure, which has to be rebuilt again, causing additional emissions. The emissions considered originate from two sources. Firstly, from permafrost carbon feedback using the estimates of its carbon pool and thawing predictions. Secondly, from infrastructure reconstruction by overlapping permafrost, settlement grid and night-time light maps to calculate the hazardous area. Then, both of them are combined and used in the model.

As a result, the estimated SCC is higher by 6-24% until 2100 than current predictions without the combined effect of permafrost and infrastructure component. By the 23rd century, the atmospheric carbon concentration is 312 ppm higher compared to the model without permafrost and infrastructure. Also, an additional temperature increase rises to 2.2°C at the end of 2300. The extra carbon concentration constitutes to additional 110 trillion US dollars of climate damages by the year 2200. Permafrost carbon feedback and infrastructure damages are of a local occurrence, but the respective emitted greenhouse gases result in global effects of irreversible and adverse climate change consequences affecting all economies globally.

The research shows that the current Social Cost of Carbon (SCC) is undervalued. The implication is that it results in stagnating technological innovations to reduce GHG emissions and exacerbating global warming. Hence, we recommend the improvement of models that estimate the SCC by including a combined permafrost and infrastructure element. Consideration of more accurate and higher SCC by policymakers and businesses can foster the world's transition to low carbon since high enough price encourages green innovation and climate investments, making them worthwhile. Moreover, the SCC in investment decisions has to increase over time to mitigate cumulative future damages due to the carbon feedback since even if global warming and additional permafrost thaw stopped today, the carbon dioxide would still be released.

6. Limitations and Future Research

The limitations of the thesis can be broadly classified into the limitation of the model and data parts. Regarding the model limitations, some researchers criticise that DICE critically underestimates the perils of climate change. For example, the damage function might be too low and does not explicitly acknowledge the prospect of low chance, high impact events. Including such events, happening at low probability but causing severe losses if they occur, will lead to more rigorous climate action. Many more economy-climate models have been formulated in the last decades, some of which are significantly more sophisticated than DICE. Moreover, many of these models focus only on particular aspects of the problem, for example, the elements of the energy sector. This is still a very active field of research. However limited DICE might be, it has laid the grounds for a highly important scientific and societal discussion. Even if one should take its specific output with a pinch of salt, it is a relevant tool to help policymakers apprehend the nature of the climate economy qualitatively. A further area of investigation would be to combine some specialised models with DICE and evaluate the results.

As per the limitation of data, the data for permafrost used for the thesis has an appropriate spatial resolution, but as technology advances rapidly and specialised satellites with even better spatial resolution take images. The procedure could be repeated with these higher quality data to arrive at even more precise results. Also, the data used for the infrastructure was two-dimensional. Several space agencies are currently working towards creating a three-dimensional model of all infrastructure on earth with LIDAR satellites. Such kind of data would result in an even more precise estimation of GHG potential from infrastructure damage. Exactly how future climate will develop is an ongoing question – one that scientists and citizens worldwide are closely monitoring. Future work and models should be adapted to what unfolds in future.

References

- Ahluwalia, M. B. (2017, September 8). *The Business of Pricing Carbon: How Companies are Pricing Carbon to Mitigate Risks and Prepare for a Low-Carbon Future*. Center for Climate and Energy Solutions.
<https://www.c2es.org/document/the-business-of-pricing-carbon-how-companies-are-pricing-carbon-to-mitigate-risks-and-prepare-for-a-low-carbon-future/>
- Anisimov, O., Fitzharris, B., Hagen, J. O., Jefferies, R., Marchant, H., Nelson, F., Prowse, T., & Vaughan, D. G. (2001). Polar regions (arctic and antarctic). *Climate Change*, 801–841.
- Asplund, D. (2017). Household Production and the Elasticity of Marginal Utility of Consumption. *The B.E. Journal of Economic Analysis & Policy*, 17(4).
<https://doi.org/10.1515/bejeap-2016-0265>
- Bento, N., & Gianfrate, G. (2020). Determinants of internal carbon pricing. *Energy Policy*, 143(C).
https://econpapers.repec.org/article/eeeeenepol/v_3a143_3ay_3a2020_3ai_3ac_3as0301421520302445.htm
- Brown, J., Jr, O. J. F., Heginbottom, J. A., & Melnikov, E. S. (1997). Circum-Arctic map of permafrost and ground-ice conditions. *Circum-Pacific Map*, Article 45. <https://doi.org/10.3133/cp45>
- Burke, E. J., Hartley, I. P., & Jones, C. D. (2012). Uncertainties in the global temperature change caused by carbon release from permafrost thawing. *The Cryosphere*, 6(5), 1063.
- Burke, E. J., Jones, C. D., & Koven, C. D. (2013). Estimating the Permafrost-Carbon Climate Response in the CMIP5 Climate Models Using a Simplified Approach. *Journal of Climate*, 26(14), 4897–4909.
<https://doi.org/10.1175/JCLI-D-12-00550.1>
- Calel, R., & Stainforth, D. A. (2017). On the Physics of Three Integrated Assessment Models. *Bulletin of the American Meteorological Society*, 98(6), 1199–1216. <https://doi.org/10.1175/BAMS-D-16-0034.1>
- Cheng, G. (2002). Interaction between Qinghai-Tibet Railway Engineering and Permafrost and Environmental Effects [J]. *Bulletin of the Chinese Academy of Sciences*, 1, 21–25.
- Cohen, J., Screen, J. A., Furtado, J. C., Barlow, M., Whittleston, D., Coumou, D., Francis, J., Dethloff, K., Entekhabi, D., & Overland, J. (2014). Recent

- Arctic amplification and extreme mid-latitude weather. *Nature Geoscience*, 7(9), 627–637.
- Collins, M., Knutti, R., Arblaster, J., Dufresne, J.-L., Fichet, T., Friedlingstein, P., Gao, X., Gutowski, W. J., Johns, T., Krinner, G., Shongwe, M., Tebaldi, C., Weaver, A. J., Wehner, M. F., Allen, M. R., Andrews, T., Beyerle, U., Bitz, C. M., Bony, S., & Booth, B. B. B. (2013). Long-term Climate Change: Projections, Commitments and Irreversibility. *Climate Change 2013 - The Physical Science Basis: Contribution of Working Group I to the Fifth Assessment Report of the Intergovernmental Panel on Climate Change*, 1029–1136.
- Companies scores—CDP*. (n.d.). Retrieved 13 December 2020, from <https://www.cdp.net/en/companies/companies-scores#446647786929955804cc9a3a08ef1eb4>
- Cramton, P., MacKay, D. J., Ockenfels, A., & Stoft, S. (Eds.). (2017). *Global Carbon Pricing: The Path to Climate Cooperation*. The MIT Press.
- DICE Model Background*. (n.d.). Retrieved 11 February 2021, from https://personal.ems.psu.edu/~dmb53/Earth_System_Models/DICE_Background.html
- DICE/RICE models—William Nordhaus | Yale Economics*. (2020, February 3). <https://sites.google.com/site/williamdnordhaus/dice-rice>
- Dutta, K., Schuur, E. A. G., Neff, J. C., & Zimov, S. A. (2006). Potential carbon release from permafrost soils of Northeastern Siberia. *Global Change Biology*, 12(12), 2336–2351.
- Earth Engine Data Catalog | Google Developers*. (n.d.). Retrieved 11 March 2021, from <https://developers.google.com/earth-engine/datasets/>
- Elberling, B., Michelsen, A., Schädel, C., Schuur, E. A., Christiansen, H. H., Berg, L., Tamstorf, M. P., & Sigsgaard, C. (2013). Long-term CO₂ production following permafrost thaw. *Nature Climate Change*, 3(10), 890–894.
- Elvidge, C. D., Baugh, K. E., Dietz, J. B., Bland, T., Sutton, P. C., & Kroehl, H. W. (1999). Radiance Calibration of DMS-OLS Low-Light Imaging Data of Human Settlements. *Remote Sensing of Environment*, 68(1), 77–88. [https://doi.org/10.1016/S0034-4257\(98\)00098-4](https://doi.org/10.1016/S0034-4257(98)00098-4)

- Elvidge, C. D., Baugh, K., Zhizhin, M., Hsu, F. C., & Ghosh, T. (2017). VIIRS night-time lights. *International Journal of Remote Sensing*, 38(21), 5860–5879. <https://doi.org/10.1080/01431161.2017.1342050>
- Elvidge, C. D., Baugh, K., Zhizhin, M., & Hsu, F. C. (2013). Why VIIRS data are superior to DMSP for mapping nighttime lights. *Proceedings of the Asia-Pacific Advanced Network*, 35, 62–69. <https://doi.org/10.7125/APAN.35.7>
- Equinor. (2020). *Equinor Sustainability Report 2019*. <https://www.equinor.com/content/dam/statoil/documents/sustainability-reports/2019/sustainability-report-2019.pdf>
- European Commission, P. O. of the E. (2018, November 28). *Communication from the Commission to the European Parliament, the European Council, the Council, the European Economic and Social Committee, the Committee of the Regions and the European Investment Bank. A Clean Planet for all A European strategic long-term vision for a prosperous, modern, competitive and climate neutral economy, COM/2018/773 final* [Website]. Publications Office of the European Union. <http://op.europa.eu/en/publication-detail/-/publication/59671a41-f3d6-11e8-9982-01aa75ed71a1/language-en>
- Falloon, P., Smith, P., Coleman, K., & Marshall, S. (1998). Estimating the size of the inert organic matter pool from total soil organic carbon content for use in the Rothamsted carbon model. *Soil Biology & Biochemistry*, 30(8–9), 1207–1211.
- Fan, J., Rehm, W., & Siccardo, G. (2021). *The state of internal carbon pricing*. <https://www.mckinsey.com/business-functions/strategy-and-corporate-finance/our-insights/the-state-of-internal-carbon-pricing#>
- Fiedler, T., Pitman, A. J., Mackenzie, K., Wood, N., Jakob, C., & Perkins-Kirkpatrick, S. E. (2021). Business risk and the emergence of climate analytics. *Nature Climate Change*, 11(2), 87–94. <https://doi.org/10.1038/s41558-020-00984-6>
- Flues, F., & Dender, K. van. (2020). *Carbon pricing design: Effectiveness, efficiency and feasibility*. <https://www.oecd-ilibrary.org/content/paper/91ad6a1e-en>
- Fu, X., & Zheng, D. (2000). Population growth and sustainable development in the Qinghai–Tibet Plateau. *Resources Science*, 22(4), 22–29.

- Garcia Duarte, P. (2008). *The Growing of Ramsey's Growth Model* (SSRN Scholarly Paper ID 1199307). Social Science Research Network. <https://papers.ssrn.com/abstract=1199307>
- Gates, B. (2021). *How to avoid a climate disaster: The solutions we have and the breakthroughs we need* (First large print edition). Random House Large Print.
- Goller, C., & Tirole, J. (2015). Negotiating effective institutions against climate change. *Economics of Energy & Environmental Policy, Volume 4*(Number 2). <https://econpapers.repec.org/article/aeneeeepjl/eeep4-2-gollier.htm>
- González-Eguino, M., & Neumann, M. B. (2016). Significant implications of permafrost thawing for climate change control. *Climatic Change, 136*(2), 381–388. <https://doi.org/10.1007/s10584-016-1666-5>
- Google Earth Engine. (n.d.). Retrieved 11 March 2021, from <https://earthengine.google.com>
- Goulden, M. L., Wofsy, S. C., Harden, J. W., Trumbore, S. E., Crill, P. M., Gower, S. T., Fries, T., Daube, B. C., Fan, S.-M., & Sutton, D. J. (1998). Sensitivity of boreal forest carbon balance to soil thaw. *Science, 279*(5348), 214–217.
- Griffies, S. M., Winton, M., Donner, L. J., Horowitz, L. W., Downes, S. M., Farneti, R., Gnanadesikan, A., Hurlin, W. J., Lee, H.-C., & Liang, Z. (2011). The GFDL CM3 coupled climate model: Characteristics of the ocean and sea ice simulations. *Journal of Climate, 24*(13), 3520–3544.
- Guo, D., & Sun, J. (2015). Permafrost thaw and associated settlement hazard onset timing over the Qinghai-Tibet engineering corridor. *International Journal of Disaster Risk Science, 6*(4), 347–358.
- Guo, D., & Wang, H. (2012). The significant climate warming in the northern Tibetan Plateau and its possible causes. *International Journal of Climatology, 32*(12), 1775–1781.
- Guo, D., & Wang, H. (2013). Simulation of permafrost and seasonally frozen ground conditions on the Tibetan Plateau, 1981–2010. *Journal of Geophysical Research: Atmospheres, 118*(11), 5216–5230.
- Guo, D., & Wang, H. (2014). Simulated change in the near-surface soil freeze/thaw cycle on the Tibetan Plateau from 1981 to 2010. *Chinese Science Bulletin, 59*(20), 2439–2448.

- Guo, D., Yang, M., & Wang, H. (2011a). Sensible and latent heat flux response to diurnal variation in soil surface temperature and moisture under different freeze/thaw soil conditions in the seasonal frozen soil region of the central Tibetan Plateau. *Environmental Earth Sciences*, *63*(1), 97–107.
<https://doi.org/10.1007/s12665-010-0672-6>
- Guo, D., Yang, M., & Wang, H. (2011b). Characteristics of land surface heat and water exchange under different soil freeze/thaw conditions over the central Tibetan Plateau. *Hydrological Processes*, *25*(16), 2531–2541.
<https://doi.org/10.1002/hyp.8025>
- Haites, E. (2018). Carbon taxes and greenhouse gas emissions trading systems: What have we learned? *Climate Policy*, *18*(8), 955–966.
<https://doi.org/10.1080/14693062.2018.1492897>
- Hare, B., Brecha, R., & Schaeffer, M. (2018). Integrated Assessment Models: What are they and how do they arrive at their conclusions? *Climate Analytics*. /publications/2018/integrated-assessment-models-what-are-they-and-how-do-they-arrive-at-their-conclusions/
- Hartmann, D. L., Tank, A. M. G. K., Rusticucci, M., Alexander, L. V., Brönnimann, S., Charabi, Y. A. R., Dentener, F. J., Dlugokencky, E. J., Easterling, D. R., Kaplan, A., Soden, B. J., Thorne, P. W., Wild, M., & Zhai, P. (2013). Observations: Atmosphere and surface. *Climate Change 2013 the Physical Science Basis: Working Group I Contribution to the Fifth Assessment Report of the Intergovernmental Panel on Climate Change*, 159–254. <https://doi.org/10.1017/CBO9781107415324.008>
- Heal, G. M., & Millner, A. (2014). Agreeing to disagree on climate policy. *Proceedings of the National Academy of Sciences*, *111*(10), 3695–3698.
<https://doi.org/10.1073/pnas.1315987111>
- Heginbottom, J., Brown, J., Ferrians, O., & Melnikov, E. S. (2002). *Circum-Arctic Map of Permafrost and Ground-Ice Conditions, Version 2* [Data set]. NSIDC. <https://doi.org/10.7265/SKBG-KF16>
- Hintermayer, M. (2020). A carbon price floor in the reformed EU ETS: Design matters! *Energy Policy*, *147*, 111905.
<https://doi.org/10.1016/j.enpol.2020.111905>
- Hong, J., Shen, G. Q., Feng, Y., Lau, W. S., & Mao, C. (2015). Greenhouse gas emissions during the construction phase of a building: A case study in

- China. *Journal of Cleaner Production*, 103, 249–259.
<https://doi.org/10.1016/j.jclepro.2014.11.023>
- Hope, C., & Schaefer, K. (2016). Economic impacts of carbon dioxide and methane released from thawing permafrost. *NATURE CLIMATE CHANGE*, 6, 6.
- Hovi, J., Sprinz, D. F., Sælen, H., & Underdal, A. (2019). The Club Approach: A Gateway to Effective Climate Co-operation? *British Journal of Political Science*, 49(3), 1071–1096. <https://doi.org/10.1017/S0007123416000788>
- Howard, P. H., & Schwartz, J. (2016). Think Global: International Reciprocity as Justification for a Global Social Cost of Carbon. *SSRN Electronic Journal*.
<https://doi.org/10.2139/ssrn.2822513>
- Hsu, F. C., Baugh, K. E., Ghosh, T., Zhizhin, M., & Elvidge, C. D. (2015). DMSP-OLS Radiance Calibrated Nighttime Lights Time Series with Intercalibration. *Remote Sensing*, 7(2), 1855–1876.
<https://doi.org/10.3390/rs70201855>
- Hugelius, G., Strauss, J., Zubrzycki, S., Harden, J. W., Schuur, E. A. G., Ping, C.-L., Schirrmeister, L., Grosse, G., Michaelson, G. J., & Koven, C. D. (2014). Estimated stocks of circumpolar permafrost carbon with quantified uncertainty ranges and identified data gaps. *Biogeosciences (Online)*, 11(23).
- Jowitt, P., Johnson, A., Moir, S., & Grenfell, R. (2012). A protocol for carbon emissions accounting in infrastructure decisions. *Proceedings of the Institution of Civil Engineers - Civil Engineering*, 165(2), 89–95.
<https://doi.org/10.1680/cien.2012.165.2.89>
- Kessler, L. (2017). Estimating the Economic Impact of the Permafrost Carbon Feedback. *Climate Change Economics*, 08(02), 1750008.
<https://doi.org/10.1142/S2010007817500087>
- Kleinen, T., & Brovkin, V. (2018). Pathway-dependent fate of permafrost region carbon. *Environmental Research Letters*, 13(9), 094001.
<https://doi.org/10.1088/1748-9326/aad824>
- Knoblauch, C., Beer, C., Sosnin, A., Wagner, D., & Pfeiffer, E.-M. (2013). Predicting long-term carbon mineralization and trace gas production from thawing permafrost of Northeast Siberia. *Global Change Biology*, 19(4), 1160–1172.

- Kolev, A., Gardner, S., European Investment Bank, & Bruegel (Organisation) (Eds.). (2012). *Investment and growth in the time of climate change*. European Investment Bank ; Bruegel.
- Koven, C. D., Riley, W. J., & Stern, A. (2013). Analysis of Permafrost Thermal Dynamics and Response to Climate Change in the CMIP5 Earth System Models. *Journal of Climate*, 26(6), 1877–1900.
<https://doi.org/10.1175/JCLI-D-12-00228.1>
- Koven, C. D., Ringeval, B., Friedlingstein, P., Ciais, P., Cadule, P., Khvorostyanov, D., Krinner, G., & Tarnocai, C. (2011). Permafrost carbon-climate feedbacks accelerate global warming. *Proceedings of the National Academy of Sciences*, 108(36), 14769–14774.
- Krichene, H. (2019). *Hazem2410/PyDICE*. GitHub.
<https://github.com/hazem2410/PyDICE>
- Kurtzer-Meyers, G. (2020, September 20). *The Future of Global Warming Lies in Data Analytics*. Medium. <https://medium.com/swlh/the-future-of-global-warming-lies-in-data-analytics-63d255d6b62c>
- Larsen, J., Mohan, S., Marsters, P., & Herndon, W. (2018). *Energy and environmental implications of a carbon tax in the United States*. 68.
- Lawrence, D. M., Slater, A. G., & Swenson, S. C. (2012). Simulation of Present-Day and Future Permafrost and Seasonally Frozen Ground Conditions in CCSM4. *Journal of Climate*, 25(7), 2207–2225.
<https://doi.org/10.1175/JCLI-D-11-00334.1>
- Li, F., Wang, H., & Gao, Y.Q. (2015). Change in sea ice cover is responsible for non-uniform variation in winter temperature over East Asia. *Atmospheric and Oceanic Science Letters*, 8(6), 376–382.
- Li, Q., & Chen, H. (2013). Variation of seasonal frozen soil in East China and their association with monsoon activity under the background of global warming. *Clim Change Res Lett*, 2, 47–53.
- Liu, J., Curry, J. A., Wang, H., Song, M., & Horton, R. M. (2012). Impact of declining Arctic sea ice on winter snowfall. *Proceedings of the National Academy of Sciences*, 109(11), 4074–4079.
- MacDougall, A. H., Avis, C. A., & Weaver, A. J. (2012). Significant contribution to climate warming from the permafrost carbon feedback. *Nature Geoscience*, 5(10), 719–721. <https://doi.org/10.1038/ngeo1573>

- Martin, R., & Kemper, A. (2010). *Carbon Pricing, Innovation, and Productivity*: 12.
- Mastrandrea, M. D. (2009). *Calculating the Benefits of Climate Policy: Examining the Assumptions of Integrated Assessment Models*. <https://trid.trb.org/view/908201>
- Metcalf, G. E., & Stock, J. (2015). *The Role of Integrated Assessment Models in Climate Policy: A User's Guide and Assessment*. Belfer Center for Science and International Affairs. <https://www.belfercenter.org/publication/role-integrated-assessment-models-climate-policy-users-guide-and-assessment>
- Michaelis, P., & Wirths, H. (2020). DICE-RD: An implementation of rate-related damages in the DICE model. *Environmental Economics and Policy Studies*, 22(4), 555–584. <https://doi.org/10.1007/s10018-020-00269-4>
- Michaelson, G. J., Ping, C. L., & Kimble, J. M. (1996). Carbon storage and distribution in tundra soils of Arctic Alaska, USA. *Arctic and Alpine Research*, 28(4), 414–424.
- Ministry of Climate and Environment. (2017, October 12). *Better growth, lower emissions – the Norwegian Government's strategy for green competitiveness* [Plan]. Government.No; regjeringen.no. <https://www.regjeringen.no/en/dokumenter/bedre-vekst-lavere-utslipp--regjeringens-strategi-for-gronn-konkurransekraft-engelsk/id2575420/>
- Mokhov, I. I., & Eliseev, A. V. (2012). Modeling of global climate variations in the 20th–23rd centuries with new RCP scenarios of anthropogenic forcing. *Doklady Earth Sciences*, 443(2), 532–536. <https://doi.org/10.1134/S1028334X12040228>
- Müller, D. B., Liu, G., Løvik, A. N., Modaresi, R., Pauliuk, S., Steinhoff, F. S., & Brattebø, H. (2013). Carbon Emissions of Infrastructure Development. *Environmental Science & Technology*, 47(20), 11739–11746. <https://doi.org/10.1021/es402618m>
- Myhre, G., Shindell, D., Bréon, F. M., Collins, W., Fuglestedt, J., Huang, J., Koch, D., Lamarque, J. F., Lee, D., Mendoza, B., Nakajima, T., Robock, A., Stephens, G., Takemura, T., & Zhang, H. (2013). Anthropogenic and natural radiative forcing. In *Climate Change 2013: The Physical Science Basis. Contribution of Working Group I to the Fifth Assessment Report of the Intergovernmental Panel on Climate Change* (T.F. Stocker, D. Qin,

- G.K. Plattner, M. Tignor, S.K. Allen, J. Doschung, A. Nauels, Y. Xia, V. Bex, and P.M. Midgley, Eds., pp. 659–740). Cambridge University Press.
- Natali, S. M., Schuur, E. A., Mauritz, M., Schade, J. D., Celis, G., Crummer, K. G., Johnston, C., Krapek, J., Pegoraro, E., & Salmon, V. G. (2015). Permafrost thaw and soil moisture driving CO₂ and CH₄ release from upland tundra. *Journal of Geophysical Research: Biogeosciences*, *120*(3), 525–537.
- National Academies of Sciences, Engineering, and Medicine. (2017). *Valuing Climate Damages: Updating Estimation of the Social Cost of Carbon Dioxide*. The National Academies Press. <https://doi.org/10.17226/24651>
- National Snow and Ice Data Center. (n.d.). *Layer: CircumArctic_Permafrost_gen25_5 (ID:5)*. Retrieved 8 April 2021, from https://services1.arcgis.com/VAI453sU9tG9rSmh/arcgis/rest/services/WorldGeo_Physical_Climate_features/FeatureServer/5
- Nelson, F. E., & Anisimov, O. A. (1993). Permafrost zonation in Russia under anthropogenic climatic change. *Permafrost and Periglacial Processes*, *4*(2), 137–148.
- Nelson, F. E., Anisimov, O. A., & Shiklomanov, N. I. (2001). Subsidence risk from thawing permafrost. *Nature*, *410*(6831), 889–890. <https://doi.org/10.1038/35073746>
- Nelson, F. E., Anisimov, O. A., & Shiklomanov, N. I. (2002). Climate change and hazard zonation in the circum-Arctic permafrost regions. *Natural Hazards*, *26*(3), 203–225.
- Nikas, A., Doukas, H., & Papandreou, A. (2019). A Detailed Overview and Consistent Classification of Climate-Economy Models. In H. Doukas, A. Flamos, & J. Lieu (Eds.), *Understanding Risks and Uncertainties in Energy and Climate Policy: Multidisciplinary Methods and Tools for a Low Carbon Society* (pp. 1–54). Springer International Publishing. https://doi.org/10.1007/978-3-030-03152-7_1
- Nitzbon, J., Westermann, S., Langer, M., Martin, L. C. P., Strauss, J., Labor, S., & Boike, J. (2020). Fast response of cold ice-rich permafrost in northeast Siberia to a warming climate. *Nature Communications*, *11*(1), 2201. <https://doi.org/10.1038/s41467-020-15725-8>

- Nordhaus, W. (2015). Climate Clubs: Overcoming Free-riding in International Climate Policy. *American Economic Review*, *105*(4), 1339–1370.
<https://doi.org/10.1257/aer.15000001>
- Nordhaus, W. (2017a). Integrated Assessment Models of Climate Change. *National Bureau of Economic Research*, *3*, 16–20.
- Nordhaus, W. (2017b). Revisiting the social cost of carbon. *Proceedings of the National Academy of Sciences*, *114*(7), 1518–1523.
<https://doi.org/10.1073/pnas.1609244114>
- Nordhaus, W. (2018). Projections and Uncertainties about Climate Change in an Era of Minimal Climate Policies. *American Economic Journal: Economic Policy*, *10*(3), 333–360. <https://doi.org/10.1257/pol.20170046>
- Nordhaus, W. (2019). Climate Change: The Ultimate Challenge for Economics. *American Economic Review*, *109*(6), 1991–2014.
<https://doi.org/10.1257/aer.109.6.1991>
- Nordhaus, W. (2020, May 29). *The Climate Club*. *99*(3). Foreign Affairs.
<https://www.foreignaffairs.com/articles/united-states/2020-04-10/climate-club>
- Nordhaus, W., & Sztorc, P. (2013). *DICE 2013R: Introduction and User's Manual*.
http://www.econ.yale.edu/~nordhaus/homepage/documents/DICE_Manual_100413r1.pdf
- Obu, J. (2021). How Much of the Earth's Surface is Underlain by Permafrost? *Journal of Geophysical Research: Earth Surface*, *126*(5).
<https://agupubs.onlinelibrary.wiley.com/doi/10.1029/2021JF006123>
- OECD. (2018). *Cost-Benefit Analysis and the Environment*. <https://www.oecd-ilibrary.org/content/publication/9789264085169-en>
- Parker, B. (2016). *The Expected Temperature Change in the Year 2100 Due to Permafrost Thawing*.
<https://ccdatacenter.org/documents/FeedbackFromPermafrost.pdf>
- Partnership for Market Readiness. (2017). *Carbon Tax Guide: A Handbook for Policy Makers*. World Bank.
<https://openknowledge.worldbank.org/handle/10986/26300>
- Peat—An overview* / *ScienceDirect Topics*. (n.d.). Retrieved 24 December 2020, from <https://www.sciencedirect.com/topics/earth-and-planetary-sciences/peat>

- Pesaresi, M., & Freire, S. (2016). *GHS-SMOD R2016A - GHS settlement grid, following the REGIO model 2014 in application to GHSL Landsat and CIESIN GPW v4-multitemporal (1975-1990-2000-2015)*.
http://data.europa.eu/89h/jrc-ghsl-ghs_smod_pop_globe_r2016a
- Porfiriev, B. N., Eliseev, D. O., & Streletskiy, D. A. (2019). Economic Assessment of Permafrost Degradation Effects on Road Infrastructure Sustainability under Climate Change in the Russian Arctic. *Herald of the Russian Academy of Sciences*, 89(6), 567–576.
<https://doi.org/10.1134/S1019331619060121>
- Price, R., Thornton, S., & Nelson, S. (2007, December). *The Social Cost of Carbon and the Shadow Price of Carbon: What they are, and how to use them in economic appraisal in the UK* [MPRA Paper]. <https://mpra.ub.uni-muenchen.de/74976/>
- Qin, D., Zhou, B., & Xiao, C. (2014). Progress in studies of cryospheric changes and their impacts on climate of China. *Journal of Meteorological Research*, 28(5), 732–746.
- Rigby, S. (2020). *Climate change: Should we change the terminology?* BBC Science Focus Magazine. <https://www.sciencefocus.com/news/climate-change-should-we-change-the-terminology/>
- Rivkin, F. M. (1998). Release of methane from permafrost as a result of global warming and other disturbances. *Polar Geography*, 22(2), 105–118.
- Roser, M. (2020). *Why did renewables become so cheap so fast? And what can we do to use this global opportunity for green growth?* Our World in Data. <https://ourworldindata.org/cheap-renewables-growth>
- Sato, M., & Schmidt, G. (n.d.). *Forcings in GISS Climate Model: Well-Mixed Greenhouse Gases RCP6.0*. National Aeronautics and Space Administration. <https://data.giss.nasa.gov/modelforce/ghgases/>
- Savaresi, A. (2016). The Paris Agreement: A new beginning? *Journal of Energy & Natural Resources Law*, 34(1), 16–26.
<https://doi.org/10.1080/02646811.2016.1133983>
- Schädel, C., Bader, M. K.-F., Schuur, E. A., Biasi, C., Bracho, R., Čapek, P., De Baets, S., Diáková, K., Ernakovich, J., & Estop-Aragones, C. (2016). Potential carbon emissions dominated by carbon dioxide from thawed permafrost soils. *Nature Climate Change*, 6(10), 950–953.

- Schädel, C., Schuur, E. A., Bracho, R., Elberling, B., Knoblauch, C., Lee, H., Luo, Y., Shaver, G. R., & Turetsky, M. R. (2014). Circumpolar assessment of permafrost C quality and its vulnerability over time using long-term incubation data. *Global Change Biology*, *20*(2), 641–652.
- Schaefer, K., Zhang, T., Bruhwiler, L., & Barrett, A. P. (2011). Amount and timing of permafrost carbon release in response to climate warming. *Tellus B: Chemical and Physical Meteorology*, *63*(2), 168–180.
- Schneider, S. H., Semenov, S., Patwardhan, A., Burton, I., Magadza, C. H. D., Oppenheimer, M., Pittock, A. B., Rahman, A., Smith, J. B., & Suarez, A. (2007). *Assessing key vulnerabilities and the risk from climate change. Climate Change 2007: Impacts, Adaptation and Vulnerability. Contribution of Working Group II to the Fourth Assessment Report of the Intergovernmental Panel on Climate Change. ML Parry, OF Canziani, JP Palutikof, PJ van der Linden, and CE Hanson, Eds.* Cambridge University Press, Cambridge, UK.
- Schneider von Deimling, T., Grosse, G., Strauss, J., Schirrmeister, L., Morgenstern, A., Schaphoff, S., Meinshausen, M., & Boike, J. (2014). Observation-based modelling of permafrost carbon fluxes with accounting for deep carbon deposits and thermokarst activity. *Biogeosciences Discussions*, *11*(12), 16599–16643.
- Schneider von Deimling, T., Meinshausen, M., Levermann, A., Huber, V., Frieler, K., Lawrence, D. M., & Brovkin, V. (2012). Estimating the near-surface permafrost-carbon feedback on global warming. *Biogeosciences*, *9*(2), 649–665. <https://doi.org/10.5194/bg-9-649-2012>
- Schuur, E. A., Abbott, B. W., Bowden, W. B., Brovkin, V., Camill, P., Canadell, J. G., Chanton, J. P., Chapin, F. S., Christensen, T. R., & Ciais, P. (2013). Expert assessment of vulnerability of permafrost carbon to climate change. *Climatic Change*, *119*(2), 359–374.
- Schuur, E. A., Bockheim, J., Canadell, J. G., Euskirchen, E., Field, C. B., Goryachkin, S. V., Hagemann, S., Kuhry, P., Lafleur, P. M., & Lee, H. (2008). Vulnerability of permafrost carbon to climate change: Implications for the global carbon cycle. *BioScience*, *58*(8), 701–714.
- Schuur, E. A., McGuire, A. D., Schädel, C., Grosse, G., Harden, J. W., Hayes, D. J., Hugelius, G., Koven, C. D., Kuhry, P., & Lawrence, D. M. (2015).

- Climate change and the permafrost carbon feedback. *Nature*, 520(7546), 171–179.
- Schuur, E. A., Vogel, J. G., Crummer, K. G., Lee, H., Sickman, J. O., & Osterkamp, T. E. (2009). The effect of permafrost thaw on old carbon release and net carbon exchange from tundra. *Nature*, 459(7246), 556–559.
- Schwanitz, V. J. (2013). Evaluating integrated assessment models of global climate change. *Environmental Modelling & Software*, 50, 120–131. <https://doi.org/10.1016/j.envsoft.2013.09.005>
- Seligman, B. J. (2000). Long-term variability of pipeline–permafrost interactions in north-west Siberia. *Permafrost and Periglacial Processes*, 11(1), 5–22.
- Slater, A. G., & Lawrence, D. M. (2013). Diagnosing Present and Future Permafrost from Climate Models. *Journal of Climate*, 26(15), 5608–5623. <https://doi.org/10.1175/JCLI-D-12-00341.1>
- Smith, B. (2020, January 16). Microsoft will be carbon negative by 2030. *The Official Microsoft Blog*. <https://blogs.microsoft.com/blog/2020/01/16/microsoft-will-be-carbon-negative-by-2030/>
- Smith, E. A., & McCarter, J. (1997). Contested Arctic: Indigenous Peoples, Industrial States, and the Circumpolar Environment. *Anthropologica*, 40(2), 230. <https://doi.org/10.2307/25605905>
- Stanton, E., Ackerman, F., & Kartha, S. (2009). Inside the integrated assessment models: Four issues in climate economics. *Climate and Development*, 1(2), 166–184. <https://doi.org/10.3763/cdev.2009.0015>
- Stavins, R. N. (2007). A U.S. Cap-and-Trade System to Address Global Climate Change. *SSRN Electronic Journal*. <https://doi.org/10.2139/ssrn.1026353>
- Stern, N., & Stiglitz, J. E. (2021). *Getting the social cost of carbon right*. Eco-Business. <https://www.eco-business.com/opinion/getting-the-social-cost-of-carbon-right/>
- Stiglitz, J. E. (2015). Overcoming the Copenhagen Failure with Flexible Commitments. *Economics of Energy & Environmental Policy*, 4(2). <https://doi.org/10.5547/2160-5890.4.2.jsti>
- Streletskiy, D. A., Suter, L. J., Shiklomanov, N. I., Porfiriev, B. N., & Eliseev, D. O. (2019). Assessment of climate change impacts on buildings, structures and infrastructure in the Russian regions on permafrost. *Environmental*

- Research Letters*, 14(2), 025003. <https://doi.org/10.1088/1748-9326/aaf5e6>
- Sustainable Prosperity. (2010). *Carbon pricing, investment, and the low carbon economy* (Policy Brief).
<http://institute.smartprosperity.ca/sites/default/files/publications/files/Carbon%20Pricing,%20Investment,%20and%20the%20Low%20Carbon%20Economy.pdf>
- Tang, S., & Demeritt, D. (2018). Climate Change and Mandatory Carbon Reporting: Impacts on Business Process and Performance. *Business Strategy and the Environment*, 27(4), 437–455.
<https://doi.org/10.1002/bse.1985>
- Tarnocai, C., Canadell, J. G., Schuur, E. A., Kuhry, P., Mazhitova, G., & Zimov, S. (2009). Soil organic carbon pools in the northern circumpolar permafrost region. *Global Biogeochemical Cycles*, 23(2).
- Than, K. (2015, January 12). *Estimated social cost of climate change not accurate, Stanford scientists say*. Stanford University.
<http://news.stanford.edu/news/2015/january/emissions-social-costs-011215.html>
- The Goldman Sachs Group. (2010). Transition to a Low-Carbon Economy. *Clean Energy*, 8.
- UNFCCC. (1997). *Kyoto Protocol* (No. 3; 3rd Conference of the Parties).
- UNFCCC. (2015). *Paris Agreement* (No. 21; 21st Conference of the Parties).
- United States Government. (2010). *Technical Support Document:-Technical Update of the Social Cost of Carbon for Regulatory Impact Analysis-Under Executive Order 12866*.
https://www.epa.gov/sites/production/files/2016-12/documents/scc_tsd_2010.pdf
- United States Government. (2016). *Technical Support Document:-Technical Update of the Social Cost of Carbon for Regulatory Impact Analysis-Under Executive Order 12866*.
https://www.epa.gov/sites/production/files/2016-12/documents/sc_co2_tsd_august_2016.pdf
- van Vuuren, D. P., Edmonds, J. A., Kainuma, M., Riahi, K., & Weyant, J. (2011). A special issue on the RCPs. *Climatic Change*, 109(1–2), 1–4.
<https://doi.org/10.1007/s10584-011-0157-y>

- Wang, Heming, Wang, Y., Fan, C., Wang, X., Wei, Y., Zhang, Z., Wang, J., Ma, F., & Yue, Q. (2020). Material Consumption and Carbon Emissions Associated with the Infrastructure Construction of 34 Cities in Northeast China. *Complexity*, 2020, 4364912. <https://doi.org/10.1155/2020/4364912>
- Wang, Huijun, Chen, H.-P., & Liu, J. (2015). Arctic sea ice decline intensified haze pollution in eastern China. *Atmospheric and Oceanic Science Letters*, 8(1), 1–9.
- Wang, Huijun, & Sun, J. (2009). Variability of Northeast China river break-up date. *Advances in Atmospheric Sciences*, 26(4), 701–706.
- Weitzman, M. L. (2017). On a World Climate Assembly and the Social Cost of Carbon. *Economica*, 84(336), 559–586. <https://doi.org/10.1111/ecca.12248>
- Williams, P. J. (1986). *Pipelines and permafrost: Science in a cold climate* (Vol. 10). McGill-Queen's Press-MQUP.
- Williams, P. J. (1995). Permafrost and climate change: Geotechnical implications. *Philosophical Transactions of the Royal Society of London. Series A: Physical and Engineering Sciences*, 352(1699), 347–358.
- WMO, UNEP, IPCC, UNESCO, & Global Carbon Project. (2020). *United In Science: A multi-organization high-level compilation of the latest climate science information*. WMO. https://library.wmo.int/doc_num.php?explnum_id=10361
- World Bank. (2017). *Report of the High-Level Commission on Carbon Prices* (High-Level Commission on Carbon Prices). <https://www.carbonpricingleadership.org/report-of-the-highlevel-commission-on-carbon-prices>
- Yang, K., Wu, H., Qin, J., Lin, C., Tang, W., & Chen, Y. (2014). Recent climate changes over the Tibetan Plateau and their impacts on energy and water cycle: A review. *Global and Planetary Change*, 112, 79–91.
- Yang, M., Nelson, F. E., Shiklomanov, N. I., Guo, D., & Wan, G. (2010). Permafrost degradation and its environmental effects on the Tibetan Plateau: A review of recent research. *Earth-Science Reviews*, 103(1–2), 31–44.
- Yi, S., Wang, X., Qin, Y., Xiang, B., & Ding, Y. (2014). Responses of alpine grassland on Qinghai–Tibetan plateau to climate warming and permafrost

- degradation: A modeling perspective. *Environmental Research Letters*, 9(7), 074014.
- Yumashev, D., Hope, C., Schaefer, K., Riemann-Campe, K., Iglesias-Suarez, F., Jafarov, E., Burke, E. J., Young, P. J., Elshorbany, Y., & Whiteman, G. (2019). Climate policy implications of nonlinear decline of Arctic land permafrost and other cryosphere elements. *Nature Communications*, 10(1), 1900. <https://doi.org/10.1038/s41467-019-09863-x>
- Zhang, T., Barry, R. G., Knowles, K., Heginbottom, J. A., & Brown, J. (1999). Statistics and characteristics of permafrost and ground-ice distribution in the Northern Hemisphere. *Polar Geography*, 23(2), 132–154. <https://doi.org/10.1080/10889379909377670>
- Zhou, B., Wen, Q. H., Xu, Y., Song, L., & Zhang, X. (2014). Projected changes in temperature and precipitation extremes in China by the CMIP5 multimodel ensembles. *Journal of Climate*, 27(17), 6591–6611.
- Zhou, B., Xu, Y., Wu, J., Dong, S., & Shi, Y. (2016). Changes in temperature and precipitation extreme indices over China: Analysis of a high-resolution grid dataset. *International Journal of Climatology*, 36(3), 1051–1066.
- Zhuang, Q., Melack, J. M., Zimov, S., Walter, K. M., Butenhoff, C. L., & Khalil, M. A. K. (2009). Global methane emissions from wetlands, rice paddies, and lakes. *Eos, Transactions American Geophysical Union*, 90(5), 37–38.
- Zimov, S. A., Davydov, S. P., Zimova, G. M., Davydova, A. I., Schuur, E. A. G., Dutta, K., & Chapin III, F. S. (2006). Permafrost carbon: Stock and decomposability of a globally significant carbon pool. *Geophysical Research Letters*, 33(20).